Final Report

Submitted to

State of Florida
Department of Transportation

Attn. Sandra Bell
Research Center
605 Suwannee Street, M.S. 30
Tallahassee, FL 32399-0450

HPR Study NO. 0831, WP # 051831
State Job NO. 99700-3587-101 Contract NO. BB-534

"Wireless Communication Spectrum Guidelines for ITS"

By

Electrical and Computer Engineering Department
University of Central Florida
Orlando FL 32816

UCF grant # 16-22-785

November 5, 1999

ABSTRACT

Various RF propagation models have been introduced for different frequency bands. These models can be characterized into two different classes. The first class is called deterministic and the second stochastic.

Both of these techniques were utilized in a recent study performed in South Florida. The study consisted of propagation measurements taken in the 2400-2483.5 MHz Instrumentation, Scientific, and Medical (ISM) frequency band. The measurements performed in the study were then put into the Hata-Okumura propagation model. The results from the Hata-Okumura model were then imported into Mathcad. The result of this was a simulation based on propagation model seeded by experimental measurements.

This simulation-based model consists of a propagation prediction model, a terrain database, and a subsystem of various Mathcad programs to simulate coverage patterns in terms of path loss and bit error rate. Simulations are presented based on the prevalent Hata-Okumura propagation model as well as the proposed propagation model.

Overall, results were well within expectations despite propagation measuring constraints. The Mathcad model has been shown to be a viable method of simulation propagation coverage. This approach towards simulation can in the near future provide a speedy and economic service to communications system design engineers.

INTRODUCTION

Propagation models aid in the development of wireless communication networks. A wireless network can be characterized by its basic components. A typical network consists of a transmitter, receiver, and the surrounding environment. Each variable in the network will effect the propagation model that can be used or developed for the given network. A model can be used for a certain frequency band to predict with a high degree of accuracy the nature of surrounding atmosphere.

There are several models that can extrapolate out to 2.4Ghz band, but we felt that the Hata-Okumura model was the most appropriate for these tests.

Propagation mechanisms such as reflection, scattering, and diffractions always need to be accounted for. This phenomenon is more profound when there is no existing line-of-sight between the transmitting and receiving antennas. Therefore a typical mobile channel is characterized by multipath reception[1].

Predictions of signal strength and propagation coverage area are vital aspects in the design of wireless communications systems. There are three basic approaches utilized in the prediction of signal strength and propagation coverage area. They consist of the empirical approach, statistical approach, and combination of both. The first approach or empirical is the easiest to implement. It requires only the use of theoretical models, however the downside is that the actual terrain is neglected. The second approach, which is the statistical approach, is the most intensive insofar as to the amount of work that is required. It however yields the more accurate results then the empirical approach. The best approach quite possibly could be a combination of both.

There are several models that can be used for this study they are the Hata-Okumura, Walfisch-Ikegami, Bullington, Elgi, Epstien-Peterson, and Longley-rice[2-5]. Propagation models can be described or relegated to two distinct classes: deterministic and stochastic. The deterministic model is useful when mulitpath is caused by a small number of paths. The stochastic model is useful when multipath is caused by a large number of paths between the transmitter and receiver. In this study we found that the most suitable model for this study was the Hata-Okumura model. This model was designed for frequencies up to 2Ghz, and hence it is adapted in this research.

HATA-OKUMURA MODEL

The Hata-Okumura model is best suited for a large cell coverage (distances up to 100 km) and it can extrapolate predictions up to the 2GHz band [1]. This model has been proven to be accurate and is used by computer simulation tools. Here is the analytical approach to the model:

$$PL = 69.55 + 26.16 \log(f) - 13.82 \log(h_t) - a(h_m) + [44.9 - 6.55 \log(h_t)] \log(d) \text{ dB}$$

$$a(h_m) = [1.1 \log(f) - 0.7] h_m - [1.56 \log(f) - 0.8] \text{ dB} \quad \text{for midsize city}$$

where f - operating frequency (MHz)

h_t - transmitting station antenna height (m)

h_m - mobile unit antenna height (m)

$a(h_m)$ - correction factor for mobile unit antenna height (dB)

d - distance from transmitting station

Using the following parameters: f = 2000 MHz, h_t = 40 m, h_m = 1.5 m, the loss predictions for this model is shown graphically in Figure 2.1.

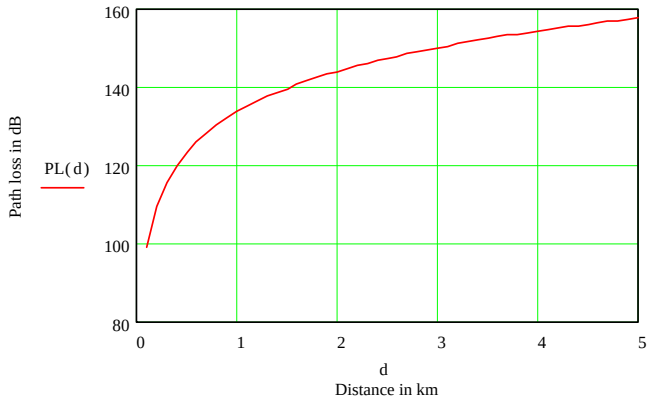

Figure 2.1 Hata-Okumura model

MATHCAD MODEL FOR POWER LOSS

To convert path loss data into a matrix format, the propagation coverage area is first viewed as a XY coordinate system. If we consider a transmitter as being located at the origin, then any position relative to this point whether occupied by a receiver or an obstruction can be defined in terms of x and y coordinates. For example, say a 5×5 km square map represents a propagation coverage area. For a 1 km grid resolution, x will take on a range of values such that $x = -5,-4.....5$ and similarly y such that $y = -5,-4.....5$. If obstructions are positioned at points (1, 4), (0, 4), (-2, 3) and (4, -2) respectively, then a mapped layout of the coverage area will be as shown in Figure 2.2.

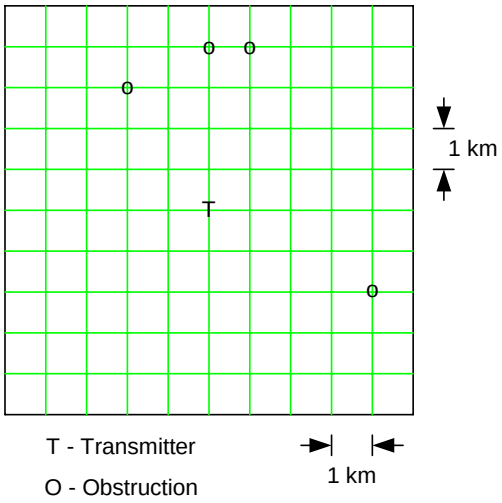

Figure 2.2 Mapped layout of propagation coverage area.

The function $fgrid(f, N)$ takes a function of two variables f as an argument and an integer N and returns a $(N+1)\times(N+1)$ grid of values of f over the square. Therefore, since a path loss equation is defined in terms of d, it is a function of x and y, and subsequently can be applied.

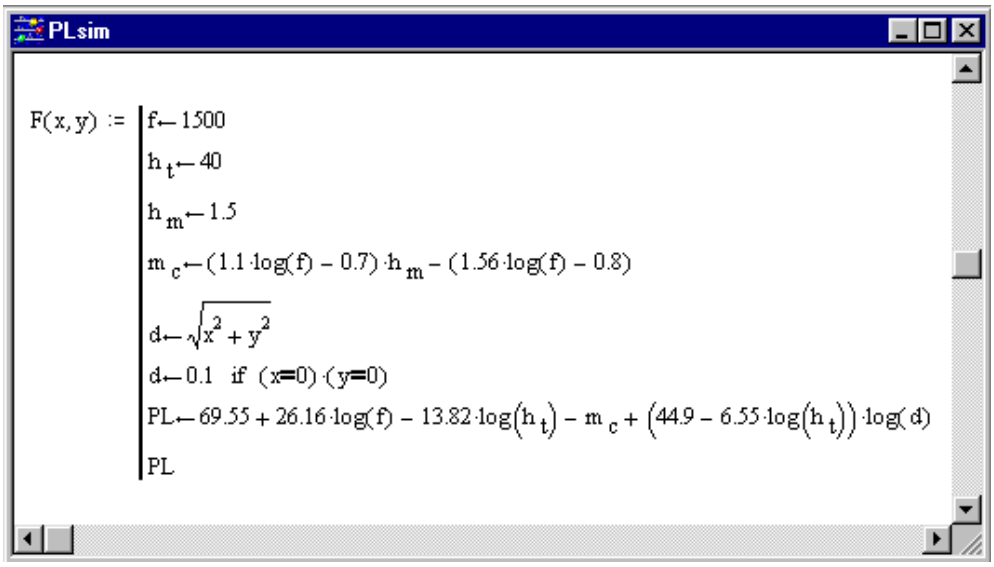

Figure 2.3 Standard formula for Hata-Okumura model as a function of x and y.

After the program is executed, an 11 × 11 matrix M is returned as shown in Figure 2.4. However, since the Hata-Okumura model ignores the effects of buildings and streets, a few building obstructions are created. These simulated buildings each represent an assumed loss of 20 dB. A data matrix Z gives their exact locations with respect to the position of the transmitter (0, 0).

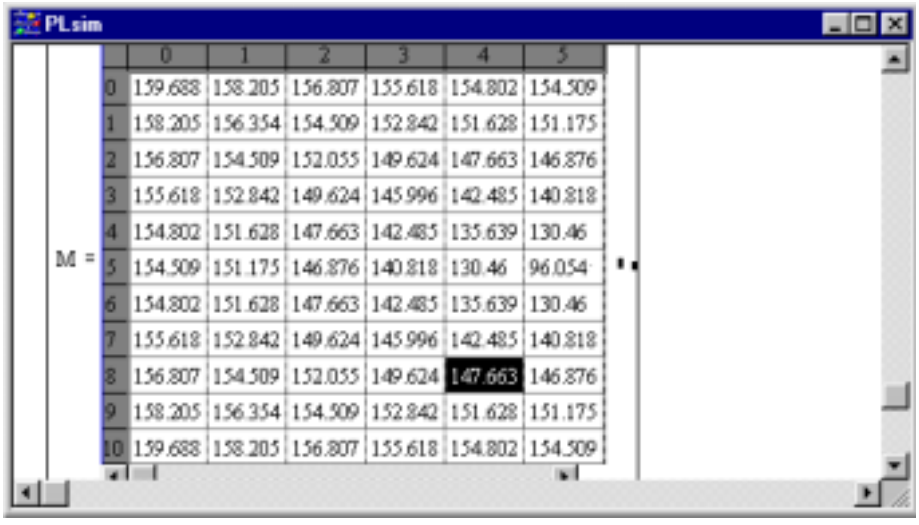

	0	1	2	3	4	5
0	159.688	158.205	156.807	155.618	154.802	154.509
1	158.205	156.354	154.509	152.842	151.628	151.175
2	156.807	154.509	152.055	149.624	147.663	146.876
3	155.618	152.842	149.624	145.996	142.485	140.818
4	154.802	151.628	147.663	142.485	135.639	130.46
5	154.509	151.175	146.876	140.818	130.46	96.054
6	154.802	151.628	147.663	142.485	135.639	130.46
7	155.618	152.842	149.624	145.996	142.485	140.818
8	156.807	154.509	152.055	149.624	147.663	146.876
9	158.205	156.354	154.509	152.842	151.628	151.175
10	159.688	158.205	156.807	155.618	154.802	154.509

Figure 2.4 Truncated 11× 11 matrix M.

The data matrix Z, as shown in Figure 2.5, actually represents simulated terrain data. However, in the real world of signal propagation this matrix will be much more detailed in terms of obstruction losses over an entire area. A typical urban environment will also require a grid resolution far greater than 1 km to simulate obstruction positions with some degree of accuracy.

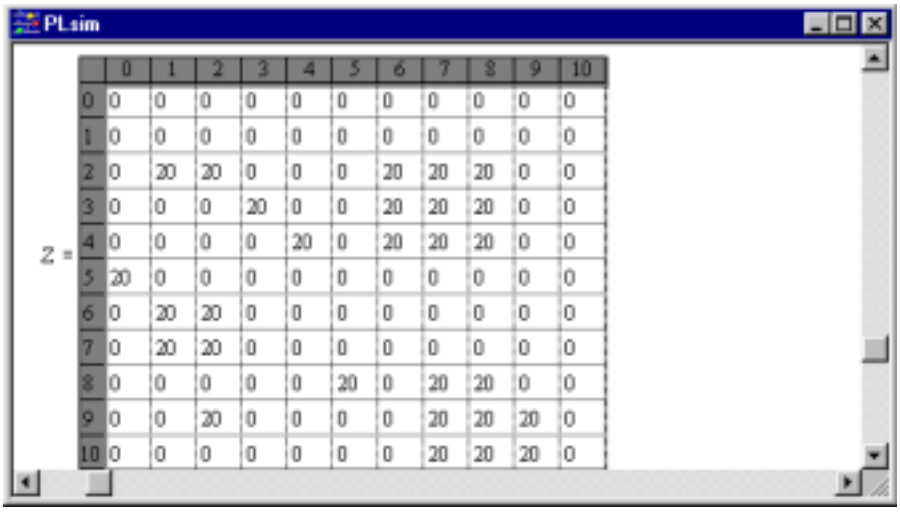

	0	1	2	3	4	5	6	7	8	9	10
0	0	0	0	0	0	0	0	0	0	0	0
1	0	0	0	0	0	0	0	0	0	0	0
2	0	20	20	0	0	0	20	20	20	0	0
3	0	0	0	20	0	0	20	20	20	0	0
4	0	0	0	0	20	0	20	20	20	0	0
5	20	0	0	0	0	0	0	0	0	0	0
6	0	20	20	0	0	0	0	0	0	0	0
7	0	20	20	0	0	0	0	0	0	0	0
8	0	0	0	0	0	20	0	20	20	0	0
9	0	0	20	0	0	0	0	20	20	20	0
10	0	0	0	0	0	0	0	20	20	20	0

Figure 2.5 Data matrix Z.

MATHCAD GENERATED SIGNAL LOSS CONTOURS

The addition of M and Z gives the total path loss matrix T. However, in order to display this result as a contour plot in its correct perspective, the T matrix needs to be fliiped around the x-axis, and its transpose is taken. These programming steps are shown in Figure 2.6.

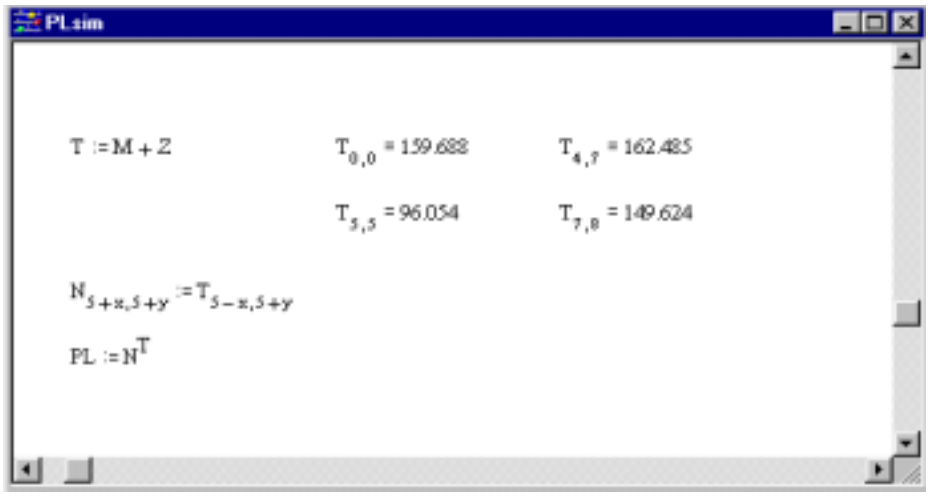

Figure 2.6 Programming steps to facilitate Mathcad default feature.

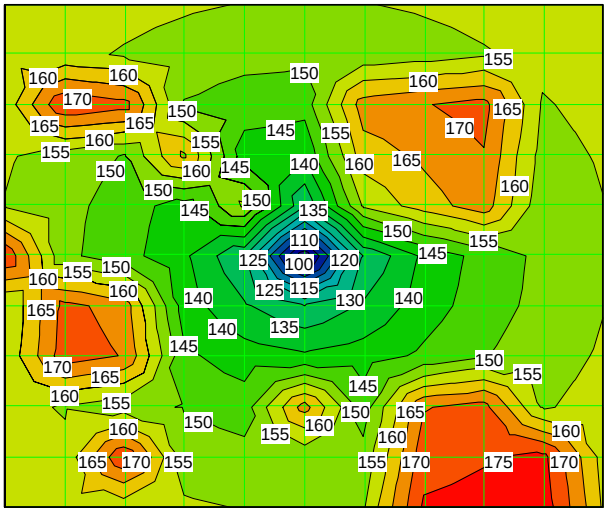

Figure 2.7 Simulated PL contour plot for the Hata-Okumura model with added obstructions.

This figure shows the simulated PL contour plot for the Hata-Okumura model with added obstructions. Using the auto contour feature, Mathcad software displays actual path loss over the 10×10 km square simulated propagation area. The apparent elastic nature of the contour lines gives a good reproduction of signal propagation around obstructions. The numbered contour lines give an indication of the path loss value in a particular region relative to the center of the grid.

MATHCAD GENERATED BER CONTOURS

The signal-to-noise ratio can be expressed as a carrier power-to-noise ratio P_rNR[6].

$$\frac{P_r}{N} = \frac{EIRP\, G_r / N}{L_s L} \tag{2.1}$$

where $EIRP$ is the transmitted signal power, and L_s is the path loss or space loss. For digital communication links it is common to replace noise power N with noise power spectral density N_o, given as

$$N_o = kT \tag{2.2}$$

where k is Boltzmann's constant (1.38×10^{-23} joule/K), and T the system effective temperature in degrees kelvin, which is a function of the noise radiated into the antenna and the thermal noise generated within the first stages of the receiver.

For BPSK modulation equation (2.1) becomes

$$\frac{P_r}{N_o} = \frac{S}{N_o} = \frac{E_b}{N_o} \cdot R_b \tag{2.3}$$

where S is the average modulating signal power, E_b/N_o the bit energy per noise power spectral density, and R_b the bit rate.

The required $\frac{E_b}{N_0}$ for BPSK modulation is found to be given by:

$$\left(\frac{E_b}{N_o}\right)_{rec} = EIRP + G_r - R_b - kT - L_s - L \tag{2.4}$$

The bit error probability for BPSK signaling is given by Sklar [7] as

$$P_b = Q\left(\sqrt{\frac{2E_b}{N_o}}\right) \tag{2.5}$$

where the Q function is defined as

$$Q(x) = 0.5\left(1 - erf\left(\frac{x}{\sqrt{2}}\right)\right) \tag{2.6}$$

The parameters used in plotting a BER curve are set as follows: P_t is is the transmitting power given as 1 W ($EIRP = P_t \cdot G_t$), and G_t the transmitting antenna gain. Note here that $(E_b/N_o)_{rec}$, expressed as $EbNoR$ in the Mathcad program is defined as a function of PL over a range of 100 to 200 dB.

Bit error probability or bit error rate (BER) may be fully understood by considering the case of a digital communication system that has at its output, a sequence of symbols. The output of the system due to the influence of channel noise (which is assumed Gaussian) will be a different sequence of bits. In an ideal or noiseless system, both input and output sequences are the same, but in a practical system, they will occasionally differ. Therefore, the bit error probability may be defined as the probability that the input sequence of symbols is not equal to the output sequence of symbols. In a practical digital communication system, the values of bit error probability range from 10^{-4} to 10^{-7}. In practice, the bit error rate (BER) is used together with time intervals to provide performance objectives for digital systems, as stated in Townsend [6].

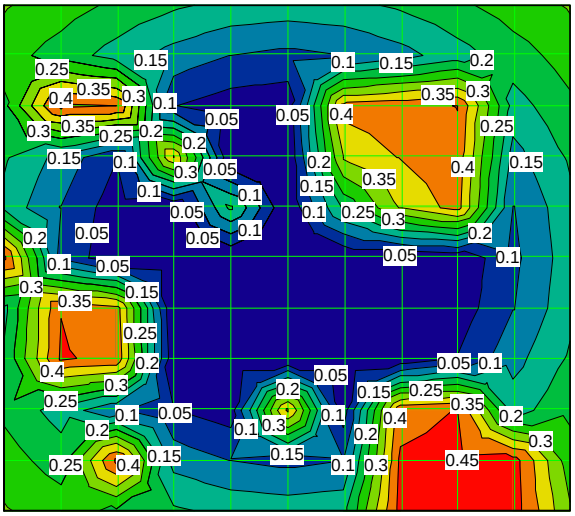

Figure 2.8 Mathcad generated BER contour plot based on the Hata-Okumura model with obstructions.

EXPERIMENTAL PATH LOSS MEASUREMENTS

In developing a RF propagation model for a DS spread spectrum communication system, radio propagation measurements (at 2.4 GHz) were taken in Dade county, Miami. A particular area called the Ives Estates was targeted for adequate propagation measurements. This urban area was somewhat close to the Golden Glades interchange (the busiest intersection in the state of Florida). These linear propagation measurements of signal strength in decibel-milliwatts (dBm) vs. distance in meters (m) were integrated into a Mathcad program in order to generate a scatter plot used in its regression analysis.

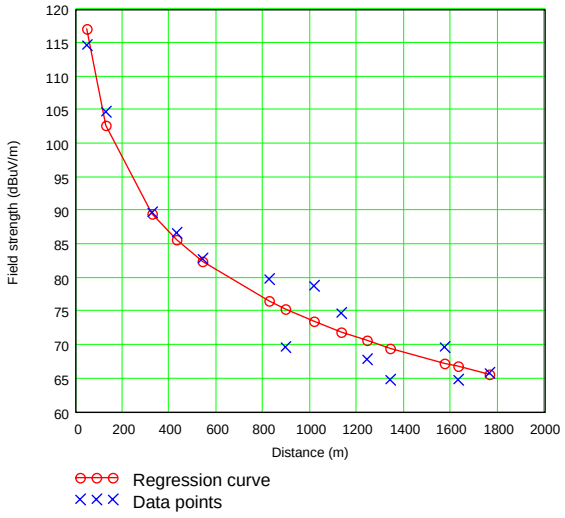

Fig. 2.9 Graphical result of the regression analysis.

For a greater degree of accuracy, the propagation coverage for the Ives Dairy Estates area is simulated using a 101×101 PL matrix. A matrix of this order results in a grid resolution of 1/10 km over a 5×5 km square map. Path loss values used in generating this matrix are obtained using the Mathcad program shown in Figure 2.10. This PL matrix as shown in Figure 2.10, gives standard path losses over the terrain as obtained by the Hata-Okumura based derivations.

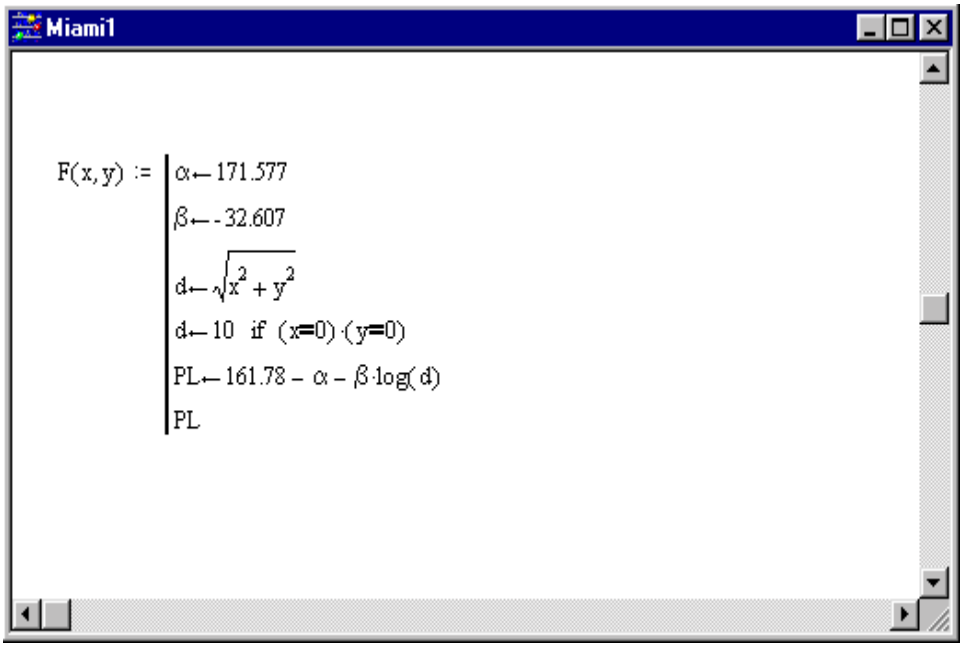

Figure 2.10 Mathcad program used in generating standard path loss values over the terrain.

A regression analysis was performed on the measured data resulting in a mean square error (MSE) of 10.75, an estimate of the error standard deviation σ, also called the standard error of estimate is given by

$$\sigma = \sqrt{MSE} \tag{2.7}$$

Based on a sample size of 10201, a vector of random numbers is generated from a normal distribution with zero mean μ and standard deviation σ, using a Mathcad built-in feature. The vector is then packed into an array of size 101×101. This new matrix B is then added to the original PL matrix M, which is defined as

$$M = fgrid(F, 100) \tag{2.8}$$

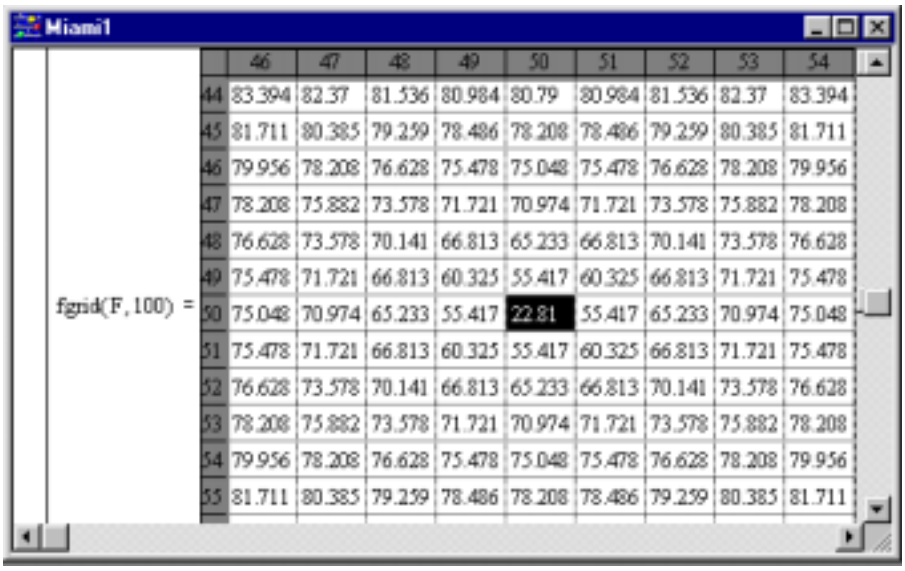

Figure 2.11 PL matrix giving standard path loss values over the terrain.

The resulting matrix S, defined in Equation (2.9), is then modified to facilitate the set of random propagation measurements taken over the terrain as defined in Figure 2.12.

$$S = M + B \tag{2.9}$$

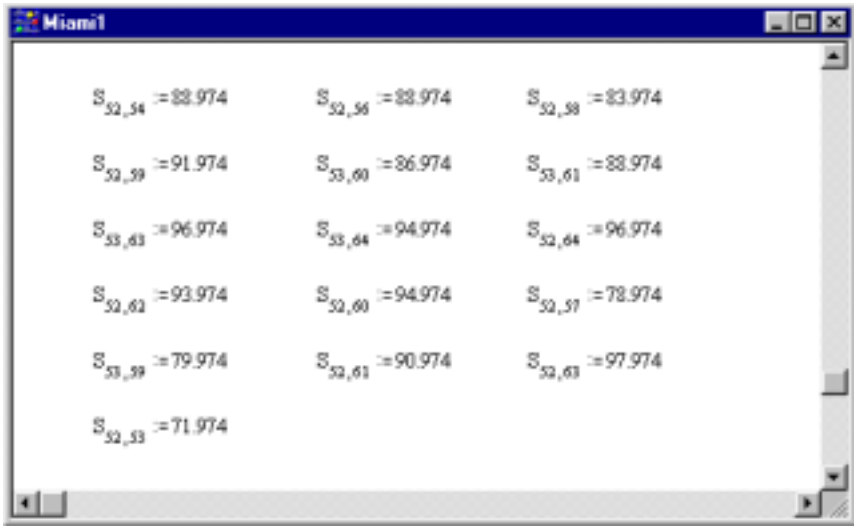

Figure 2.12 Random propagation measurements defined as path loss values.

This matrix S, taken as the final path loss matrix is plotted as shown in Figure 2.13. This simulation of the propagation coverage gives an idea of the path loss in unmeasured areas as well, based on previous analysis. However, in the specific area in question, that is the Ives Dairy road, values of path loss derived based on the random propagation measurements were in the vicinity of those proposed by regression analysis. This indicates that the proposed propagation model is well within acceptable limits. However, recalling that all propagation measurements taken were based on line-of-sight, other

propagation measurements are needed based on variable field parameters such as transmitting and receiving antenna heights and speed of the mobile unit.

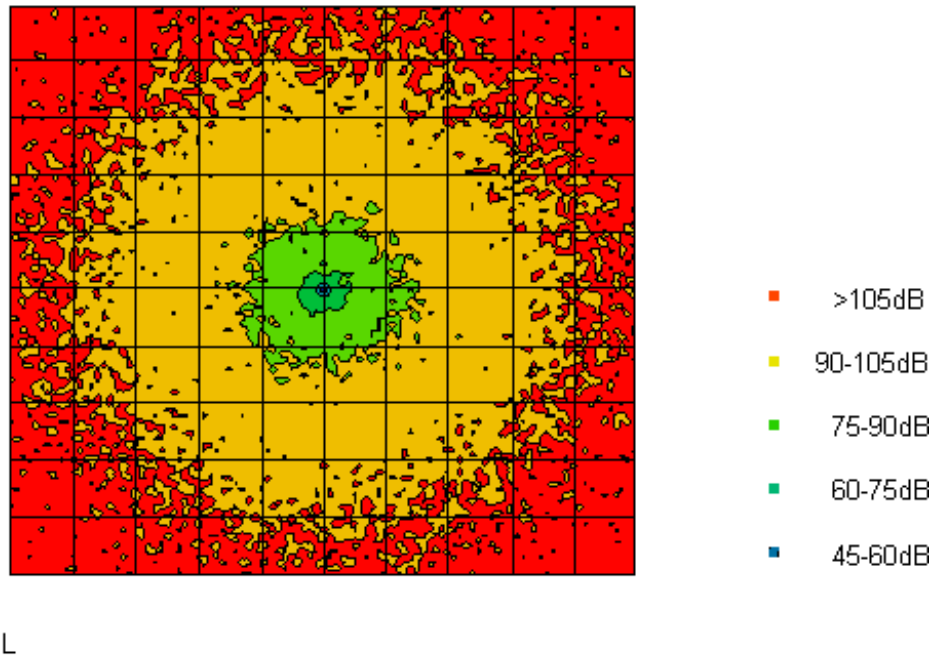

Figure 2.13 Propagation coverage simulation based on field measurements.

CONCLUSION

It is paramount when doing any communication system design that modeling of the RF propagation is accurate. For this cause, any propagation model should be optimized for its own particular environment. The prediction model presented based on the Miami propagation measurements, should be improved. Propagation measurements are needed for every facet of radio coverage, such as with variable transmitting and receiving antenna heights, with the effects of clutter, and the effects of buildings. As such the path loss constants obtained using regression analysis can be optimized, resulting in an established path loss empirical formula.

The Mathcad model has been shown to be practical method of simulating propagation coverage. However, if propagation coverage is limited to the microcell level, say 1 x 1 km square map, a 101 x 101 path loss matrix will result in a grid resolution of 1/50 km or 20 meters, producing far more accurate simulations. Overall, this Mathcad model approach can in the future provide a speedy and economic service to communications system design engineers.

LIST OF REFERENCES

1. T. S. Rappaport, “Wireless Communications: Principles and Practice,” IEEE Press, Prentice-Hall, New Jersey, 1996.

2. B.H. Fleury and P.E. Leuthold, ‘Radiowave Propagation in Mobile Communications: An Overview of European Research’. IEEE Comm. mag., Vol. 34, February 1996.

3. M. Hata, “Empirical Formula for Propagation Loss in Land Mobile Radio Services,” IEEE Trans. on Veh. Technol., vol. VT-29, pp. 317-325, August 1980.

4. A. G. Longley and P. L. Rice, “Prediction of Tropospheric Radio Transmission Loss Over Irregular Terrain: A Computer Method,” ESSA Tech. Rep. ERL 79 – ITS 67, US Govt. Printing Office, Washington DC, 1968.

5. J. Walfisch and H. L. Bertoni, “A Theoretical Model of UHF Propagation in Urban Environments,” IEEE Trans. on Antennas Propagat., vol. 36, pp. 1788-1796, December 1988.

6. A. A. R. Townsend, “Digital Line-of-sight Radio Links: A Handbook,” Prentice-Hall, London, 1988.

7. B. Sklar, “Digital Communications: Fundamentals and Applications,” Prentice-Hall, New Jersey, 1988.

APPENDIX

Details for
“Wireless Communication Spectrum Guidelines for ITS”

TABLE OF CONTENTS

LIST OF TABLES

LIST OF FIGURES

ABSTRACT

The purpose of this research is to develop a RF propagation model for direct sequence spread spectrum communication systems. The recent upsurge of digital wireless communication systems using spread spectrum technology has lead to a desire to better understand the propagation characteristics of the environment. The proposed propagation model is derived from a set of propagation measurements taken in Miami utilizing the 2400-2483.5 MHz frequency band allotted for commercial spread spectrum users. Miami is a built-up urban environment and as such multipath effects and fading are key issues.

A Mathcad model approach is proposed for presenting all propagation coverage results. This simulation-based model consists of a propagation prediction model, a terrain database, and a subsystem of various Mathcad programs to simulate coverage patterns in terms of path loss and bit error rate. Simulations are presented based on the prevalent Hata-Okumura propagation model as well as the proposed propagation model. MapInfo and ComStudy are used in the analysis of all simulated results.

Overall, results were well within expectations despite propagation measuring constraints. The Mathcad model has been shown to be a viable method of simulating propagation coverage. This approach towards simulation can in the near future provide a speedy and economic service to communications system design engineers.

CHAPTER 1

INTRODUCTION

In the mobile radio environment, a part of the electromagnetic energy radiated by the antenna of the transmitting station reaches the receiving station by propagating through different paths. Along these paths interactions commonly referred to as propagation mechanisms may occur. Possible interactions are diverse reflection on large flat surfaces, diffuse scattering from surfaces exhibiting small irregularities or from objects of small size, multiple diffraction due to knife-edge type obstacles or possible rounded objects and shadowing. The latter phenomenon is more profound when there is no existing line-of-sight between the transmitting and receiving antennas. A typical mobile channel is therefore characterized by multipath reception.

Predictions of signal strength and propagation coverage area are vital aspects in the design of mobile radio systems. There are basically three approaches used in obtaining received radio signal strengths [1]. The first, the empirical model approach is by far the simplest, however its only shortfall is that it does not adequately consider local terrain features, which determine characteristics of radio propagation. The second, the measured data approach is very tedious and time consuming, especially in large cities and

vast rural areas. This approach is considered on the other hand very practical in areas where radio coverage poses difficulty. The last approach happens to be a combination of the previously mentioned approaches. Here theoretical models are used and appropriately adapted to a local environment based on selected radio signal measurements.

From previous research results, propagation loss shows a particular logarithmic behavior to the distance [2]. Bearing this in mind and the third above-mentioned approach, one can easily adapt a prevalent model such as the Hata-Okumura model to suit a particular mobile radio environment. The Hata-Okumura model has widespread use in land mobile communications [3]. It is based on an extensive experimental study of propagation loss over different terrain within a frequency range of 100 to 1500 MHz. It predicts path loss as a function of a path loss exponent. In Chapter 2, the Bullington, Hata-Okumura and Walfisch-Ikegami propagation models are presented with a bias towards land mobile communications. Older models like Egli, Epstein-Peterson and Longley-Rice are mentioned on a purely theoretical basis.

In this research presentation, the Hata-Okumura model is used as the basis of deriving a suitable RF propagation model for the spread spectrum environment. Spread spectrum results in efficient spectrum use, and today the FCC designated frequency band of 2400-2483.5 MHz is widely used in digital cellular radios, wireless local area networks, personal communication networks, traffic control systems and global positioning systems to name a few. Spread spectrum signals are basically wide-band noise-like signals. They are categorized as either of the type ‘Direct Sequence’ or ‘Frequency Hopping’ or a combination of these two types called a hybrid [4].

This thesis highlights the direct sequence spread spectrum system, which has a few advantages, over the frequency hopping type. However, the direct sequence system requires a linear signal path for a reduced bit error probability [5]. It is this requirement that poses a problem in the real world of mobile communications, where multipath effects are always present. As a result of multipath propagation, fading occurs, since the transmitted signal becomes time dispersed. Multipath fading can produce intersymbol interference, creating bit errors at the receiver. Spread spectrum communications is discussed in detail in Chapter 3.

For this research, all radio propagation measurements were taken in Dade county, Miami, a built-up urban area with many overpasses including the popular Golden Glades interchange. A fixed transmitting station consisted of a HP8648C Signal Generator with 14.5 dBm signal strength at 2.4 GHz, along with a 12 dB gain directional antenna. The mobile unit included a HP8596E Spectrum Analyzer, a HP85901A Power Supply and likewise a 12 dB gain directional antenna. Since two directional antennas were used in the actual propagation of the 2.4 GHz signal, one had to make sure that the antennas were properly panned to reduce pointing losses.

Linear propagation measurements were taken along Alligator alley, a straight stretch of highway I-75. This measured data of signal strength vs. distance was integrated into Mathcad and used in deriving a suitable estimated logarithmic curve based on regression analysis. A devised Mathcad program calculates distance in meters between two geographical locations using global positioning system (GPS) radio measurements of longitude and latitude. Similar Mathcad programs simulate a 101×101 path loss matrix

based on the derived estimated curve. Using selected measured data from the Ives Estates, an area close to the Golden Glades interchange, as terrain data, a computer prediction of the radio path profile in terms of path loss is presented in Mathcad using contour plotting graphing techniques. The complete Mathcad model, which includes simulations done using the Hata-Okumura model, is presented in Chapter 4. A map giving the exact location of Ives Estates and the Golden Glades interchange is shown below in Figure 1.1.

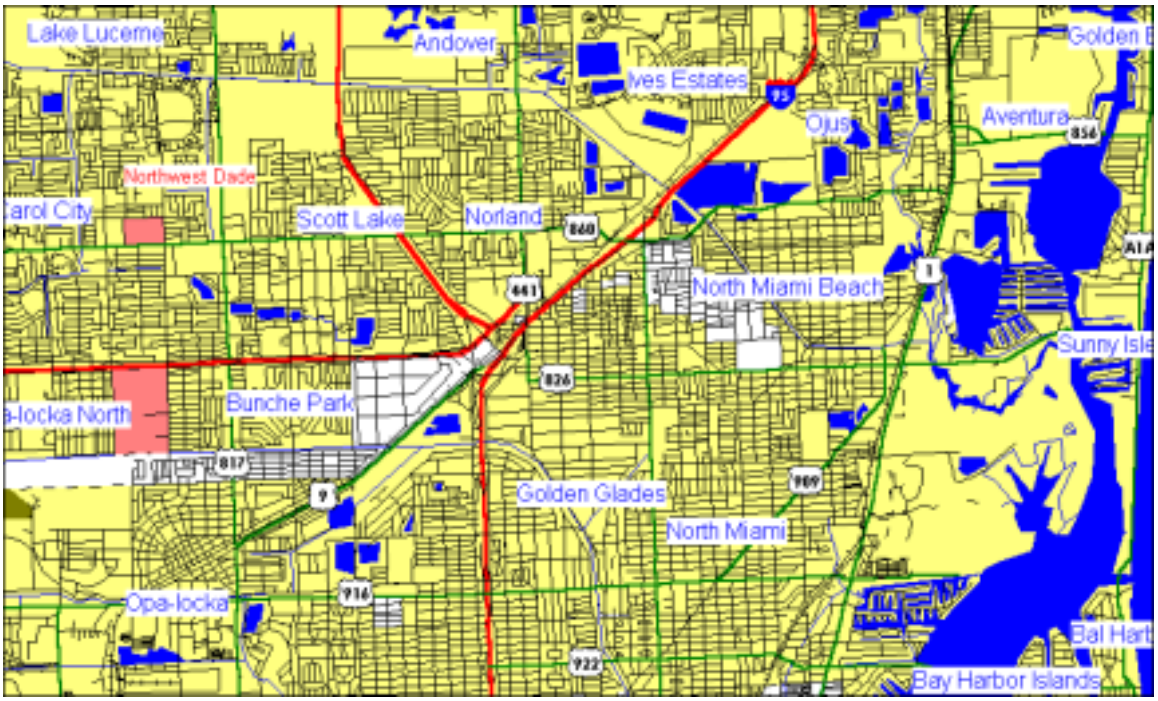

Figure 1.1 Map of the Ives Estates area and the Golden Glades interchange.

MapInfo, a desktop mapping software recommended by most communications system designers and ComStudy RF propagation software are both used in the analysis of simulated results. Chapters 5 and 6 respectively cover this aspect of the research.

In Chapter 7, a few guidelines for future work on the proposed propagation model, along with concluding statements and general comments are given with respect to the Mathcad model approach.

CHAPTER 2

PROPAGATION MODELS

A propagation model predicts mean field strength or path loss for an arbitrary transmitter-receiver separation distance. Factors affecting the mean path loss include transmitting station and mobile unit antenna heights, operating frequency, multipath effects and atmospheric conditions. Over the years, a number of attempts at predicting the mean path loss in land mobile radio environment have been made. These include the Bullington model, Hata-Okumura model and the Walfisch-Ikegami model, all of which are presented later in this chapter.

Models are basically divided into two distinct classes namely deterministic and stochastic. The deterministic model corresponds to a deterministic description of the environment that causes path loss and multipath effects, and it is useful when multipath is caused by a small number of paths that can be accurately characterized. The stochastic model corresponds to a statistical model of the environment and it is most appropriate when the multipath effects are caused by a large number of paths between transmitter and receiver that would be impossible to characterize in a deterministic way. Examples of stochastic models are the Egli model and the Bullington model, while on the other hand

the Hata-Okumura model and the Walfisch-Ikegami model are typical deterministic models.

2.1 Fundamentals of Radio Wave Propagation

Let us consider an antenna of known dimensions. If a current flows through such an antenna, it launches electric and magnetic fields based on electromagnetic theories. In electromagnetic radiation, the mode of propagation is the transverse wave; that is, waves are propagated in the direction that is perpendicular to their motion. In radio propagation however, we refer to these transverse waves as electromagnetic waves or simply radio waves. A radio wave in three-dimensional space consists of two component waves [6]. These are the electrostatic or electric component E and the magnetic component H. Note at this point that these components are orthogonal.

A radio wave is polarized in the direction of its electric component. A dipole radiator (antenna) aligns itself to the E field and thus indicates the direction of polarization; that is, vertically oriented dipole indicates vertical polarization. A typical transmitting station can either utilize horizontal polarization in an effort to have propagated radio waves cover a horizontal arc as per antenna pattern or vertical polarization as in the case of an array of vertically polarized antennas to cover selected horizontal areas.

Finally, radio waves may be propagated about the earth differently, based on a particular communications system design. Two main routes which they may travel from the transmitting antenna to the receiving antenna are either the ionosphere (sky wave), or

by hugging the ground (ground wave). In land mobile communications, the ground wave is of most importance.

2.1.1 Ground Waves

Ground waves cover those waves that are not influenced by the ionosphere, that is the surface and the space wave [6]. For the space wave, three paths may be used to traverse the distance between the transmitting antenna and the receiving antenna; namely, the direct wave or line-of-sight wave, the ground-reflected wave and the tropospherically reflected wave.

2.1.1.1 Surface Wave

In surface wave propagation, the wave energy glides over the Earth's surface as the name implies. However this mode of propagation is only useful for the transmission of radio frequencies lower than 30 MHz, since the Earth's attenuation properties increases rapidly with frequency and attenuation here depends upon the effective conductivity and dielectric constant of the Earth.

2.1.1.2 Space Wave

This mode of propagation is applicable to land mobile communications if we consider a typical radio wave in this scenario as being limited to 10 miles above the Earth's surface or the troposphere. One type of space wave, the direct wave, travels

directly from the transmitting antenna to the receiving antenna, without any reflections whatsoever. Under normal conditions, it has the greatest received magnitude.

The second type of space wave, the ground reflected wave, arrives at the receiving antenna after being reflected one or more times from the ground or surrounding objects. The reflection does not have to occur only in the vertical plane, but may occur in the horizontal plane, such as that reflected from an obstruction, offset from the main path. The reflected wave will differ in phase and amplitude than that of the direct wave, and if its distance traveled is greater by an odd number of wavelengths, its phase will be 180^{o} with respect to the direct wave at the receiving antenna. This will lead to some amount of cancellation of the direct wave at this point. The extent to which the direct wave is canceled depends on the amplitude of the reflected wave.

The third type of space wave, the troposherically reflected wave, depends on the refractive index of the air at various transmitting antenna heights above the Earth's surface. This wave may be diffracted or totally reflected from the troposphere, depending on the angle at which it was launched. It is interesting to note at this point that the troposphere can behave as a giant reflector. If a space wave happens to reach the receiving antenna, it may cancel to some extent the direct wave if they are changes in its phase and amplitude.

2.2 Free Space Propagation Model

The concept of free space assumes a channel free of all hindrances to RF propagation, such as absorption, reflection, refraction, or diffraction. The RF energy

arriving at the receiver is therefore assumed to be a function only of distance from the transmitter. A free space channel therefore characterizes an ideal RF propagation path. In practice, most propagation models are based on a modified free space propagation model.

Rappaport [3], states that the free space power received by a receiver antenna which is separated from a radiating transmitter antenna by a distance d, is given by the Friis free space equation,

$$P_r(d) = \frac{P_t G_t G_r \lambda^2}{(4\pi)^2 d^2 L} \tag{2.1}$$

where P_t is the transmitted power, $P_r(d)$ is the received power which is a function of the transmitter-receiver separation, G_t is the transmitting antenna gain, G_r is the receiving antenna gain, d is the transmitter-receiver distance in meters, L is the system loss factor not related to propagation $(L \geq 1)$, and λ is the wavelength in meters. The gain of an antenna is related to its effective aperture, A_e, by

$$G = \frac{4\pi A_e}{\lambda^2} \tag{2.2}$$

The effective aperture A_e is related to the physical size of the antenna, and λ is related to the transmitting frequency by Equation (2.3), where f is the transmitting frequency in hertz, and c is the speed of light in meters/s.

$$\lambda = \frac{c}{f} \tag{2.3}$$

Note that the miscellaneous losses L are usually due to transmission line attenuation, filter losses, and antenna losses in the communication system. A value of $L = 1$ indicates no loss in the system hardware.

The Friis free space equation of (2.1) shows an inverse square relationship between the measured power and the transmitter-receiver separation distance. This implies the received power decays at a rate of 20 dB/decade with distance.

The path loss is defined as the difference between the effective transmitted power and the received power and may include the effect of the antenna gains. The path loss PL in decibels for the free space model is given by

$$PL = -10 \log_{10} \frac{P_r}{P_t} = -10 \log_{10} \left[\frac{G_t G_r \lambda^2}{(4\pi)^2 d^2 L} \right] \tag{2.4}$$

Let us consider an ideal case of free space propagation with no system losses, that is $L = 1$, and assume ideal antennas. An isotropic radiator is considered an ideal antenna, as it radiates power with unity gain uniformly in all directions. Therefore if $G_t = G_r = 1$ and $L = 1$, Equation (2.4) becomes Equation (2.5). Substituting both Equation (2.3) and c as 3×10^8 meters/s gives Equation (2.6). For f in MHz and d in km, Equation (2.6) becomes Equation (2.7). Simplifying the last equation results in Equation (2.8).

$$PL = -10\log_{10}\left[\frac{\lambda^2}{(4\pi)^2 d^2}\right] \tag{2.5}$$

$$PL = -10\log_{10}\left[\frac{3\times10^8}{4\pi f d}\right]^2 \tag{2.6}$$

$$PL = -20\log_{10}\left(\frac{3\times10^8}{4\pi\times10^9}\right) + 20\log_{10}(f) + 20\log_{10}(d) \tag{2.7}$$

$$PL(d) = 32.4 + 20\log(f) + 20\log(d) \tag{2.8}$$

Figure 2.1 shows a plot of path loss vs. distance for the model represented by Equation (2.8). The shape of this path loss curve is a prominent feature in the analysis of other propagation models. However this model has one limitation, it is only a valid predictor of P_r for values of d which are in the far field of the transmitting antenna. The far field region is defined as the region beyond the far field distance d_f given by Equation (2.9) where D is the largest physical linear dimension of the antenna. Note that $d_f \gg D$ and likewise $d_f \gg \lambda$ are also conditions to be satisfied.

$$d_f = \frac{2D^2}{\lambda^2} \tag{2.9}$$

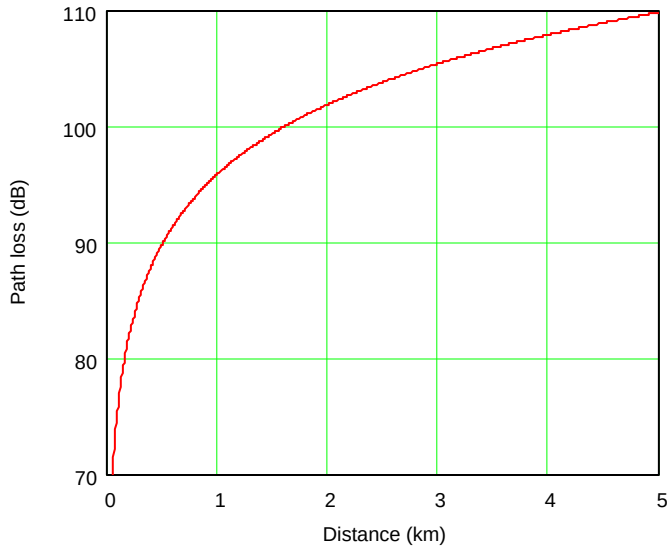

Figure 2.1 Free space propagation at 1500 MHz

2.3 Propagation Mechanisms

In reality, if we consider the effects of the Earth's surface, the expression for received power given in Equation (2.1) becomes much more complicated. The actual mechanisms that govern radio propagation are truly complex and diverse, and they can generally be attributed to three basic propagation mechanisms: reflection, diffraction, and scattering. Figure 2.2 illustrates these mechanisms in a typical urban link.

2.3.1 Reflection

Reflection occurs when a propagating electromagnetic wave impinges upon an object of large dimensions when compared to the incident wavelength. Reflections from

the surface of the Earth and from buildings or walls produce reflected waves, which may interfere either constructively or destructively at the receiver.

In essence, when an electromagnetic wave or simply a radio wave propagating in one medium impinges upon another medium having a different dielectric constant, permeability, or conductivity, the wave becomes part reflected and part transmitted. From physics, if a plane wave is incident on a perfect dielectric, part of the energy is reflected, and there is no loss of energy in absorption. On the other hand, if a plane wave is incident on a perfect conductor, the wave will be completed reflected without loss of energy.

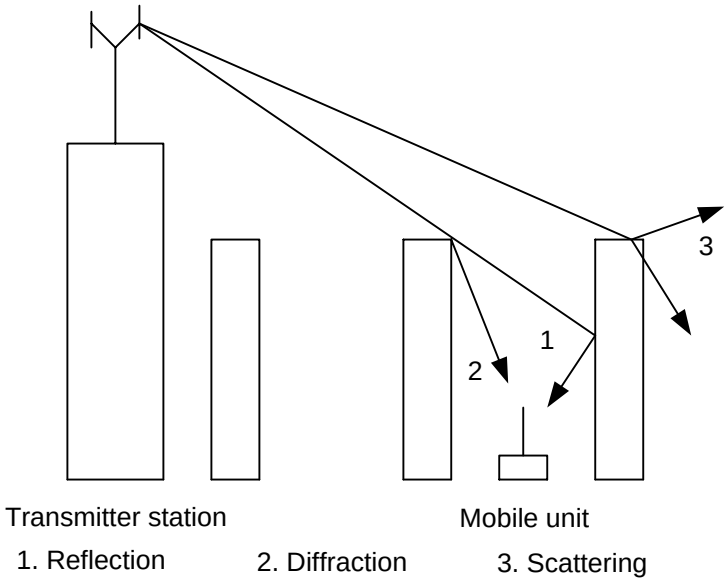

Figure 2.2 An example of the three basic propagation mechanisms in an urban environment.

Rappaport [3] mentions that the electric field intensity of the reflected wave and the incident wave are related through the Fresnel reflection coefficient Γ. The reflection coefficient is a function of the permittivity of the ground, wave polarization, angle of incidence, and the frequency of the propagating wave. Within the horizon there will be a phase delay associated with Γ, therefore the reflected ray can be expressed as a time difference, known as the difference in propagation delay [6]. It is this propagation delay that results in the part cancellation of the direct wave, mentioned in Section 2.1.1.2, and subsequent fading. The value of Γ will fluctuate in time as a consequence of variations in either the surface shape or atmospheric conditions or both. Note at high frequencies or short wavelengths, a small irregularity in the surface will appear to be larger than at lower frequencies.

Figure 2.3 shows a typical radio path within the horizon, where d_r represents the direct or line-of-sight ray, and g_r the ground reflected ray, which is itself comprised of incident and reflected rays. The angle of incidence θ_i is given as the angle between the tangent plane and the incident ray. The angle of reflection θ_r is given as the angle between the tangent plane and the reflected ray.

Let us at this point consider the case when the first propagation medium is free space and both the first and second mediums of the incident ray have similar permeability values. The reflection coefficients for the two cases of vertical and horizontal polarization can be presented as Equations (2.10) and (2.11) respectively, as given in Rappaport [3], where ε_r is the relative permittivity of the Earth.

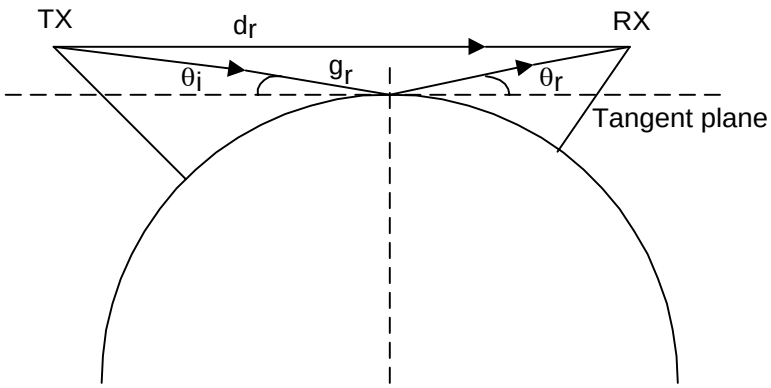

Figure 2.3 Radio path within the horizon.

$$\Gamma_v = \frac{-\varepsilon_r \sin\theta_i + \sqrt{\varepsilon_r - \cos^2\theta_i}}{\varepsilon_r \sin\theta_i + \sqrt{\varepsilon_r - \cos^2\theta_i}} \tag{2.10}$$

$$\Gamma_h = \frac{\sin\theta_i - \sqrt{\varepsilon_r - \cos^2\theta_i}}{\sin\theta_i + \sqrt{\varepsilon_r - \cos^2\theta_i}} \tag{2.11}$$

It can be shown that for an incident angle close to 0 the reflection coefficient tends to -1, independent of the polarization.

2.3.2 Diffraction

Diffraction occurs when the radio path between the transmitter and receiver is obstructed by a surface that has sharp irregularities or edges. Based on Huygen's theory [3], secondary waves are formed behind the obstructing body even though there is no

line-of-sight path between the transmitter and the receiver. Therefore, diffraction explains how a radio frequency signal can travel in urban and rural environments without an existing line-of-sight path. Shadowing a definitive term used in mobile communications also falls under the subject of diffraction. In shadowing the diffracted field can reach a receiver even when it is shadowed by an obstruction. Experiments reported by Egli in 1957 showed that, for paths longer than a few hundred meters, the received power fluctuates with a 'log-normal' distribution about the area-mean power. This normal distribution or Gaussian distribution is perhaps the most prevalent distribution in statistics.

In practice, diffraction of radio waves is the bending of the waves around objects. The amount of bending increases as the object thickness is reduced and also as the length of the wave increases. The sole reason why diffraction concerns the communications system designer is that obstructions, which are not necessarily in the direct path of the radio beam, may cause the beam to become attenuated. This attenuation is due to 'diffraction losses'.

2.3.2.1 Fresnel Zone Theory

Fresnel zones play a critical part in diffraction; they are ellipsoids surrounding the direct ray from the transmitting antenna to the receiving antenna. The first ellipsoid has the locus of its outer shell such that any signal reaching the receiving antenna via this path will travel half the transmitting wavelength more than the signal traveling via the

direct path. It is this region inside the first ellipsoid that is called the first Fresnel zone. Figure 2.4 illustrates a typical path profile showing the first Fresnel zone.

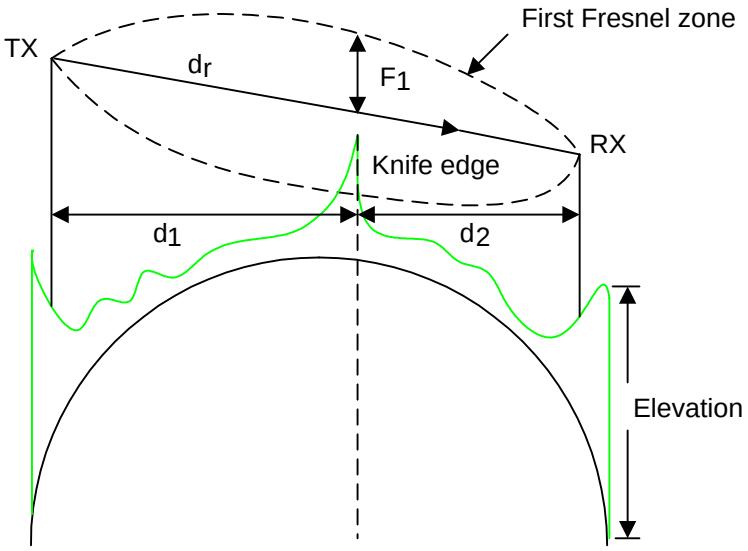

Figure 2.4 Typical path profile showing first Fresnel zone and knife-edge obstruction.

The first Fresnel zone contains most of the power that reaches the receiver. If an obstruction exists at the edge of this zone, the reflected wave will tend to cancel the direct wave. The extent of cancellation will depend on the relative amplitude of the reflected and direct waves. Besides the first Fresnel zone, there is a family of ellipsoids surrounding this first shell. These are the second; third, fourth, etc., Fresnel zones. They however have little effect in producing noticeable diffraction loss due to the signal power contained within them, being so small. For all practical purposes 60% of the first Fresnel

zone is considered clear. The radius F_n of any ellipsoid about the direct path varies along the propagation path, and is given by

$$F_n = \sqrt{\frac{n\lambda d_1 d_2}{d}} \tag{2.12}$$

where n is the Fresnel zone order; λ the wavelength of the transmitting frequency; d_1 the distance between one terminal, either transmitting or receiving, to the other point where the Fresnel zone radius is being calculated; d_2 the distance from the other terminal to the point where the Fresnel zone radius is being calculated; and d the sum of distances d_1 and d_2. The first Fresnel zone radius in meters is given by

$$F_1 = 17.32\sqrt{\frac{d_1 d_2}{fd}} \tag{2.13}$$

for d_1, d_2 and d in km, and f the transmitting frequency in GHz.

2.3.2.2 Knife Edge Diffraction

When a single object such as a hill causes shadowing, it is instructive to treat the object as a knife-edge to estimate the amount of diffraction losses. The field strength E_d, of a knife-edge-diffracted wave is given by Equation (2.14), where E_0 is the free space field strength in the absence of the knife-edge and $F(\nu)$ is the complex Fresnel integral

[7]. This integral is a function of the Fresnel-Kirchoff diffraction parameter ν, which is defined as

$$\nu = h\sqrt{\frac{2(d_1 + d_2)}{\lambda d_1 d_2}} = \alpha\sqrt{\frac{2 d_1 d_2}{\lambda(d_1 + d_2)}} \tag{2.14}$$

where h is the height of the knife-edge; d_1 and d_2 are the distances of the knife-edge from the transmitter and receiver, respectively; and α is the angle of diffraction, in radians. Depending on where the knife-edge protrudes, that is above or below the line-of-sight, h and ν will both be negative or positive respectively. Figure 2.5 illustrates a single knife-edge obstruction over an irregular terrain.

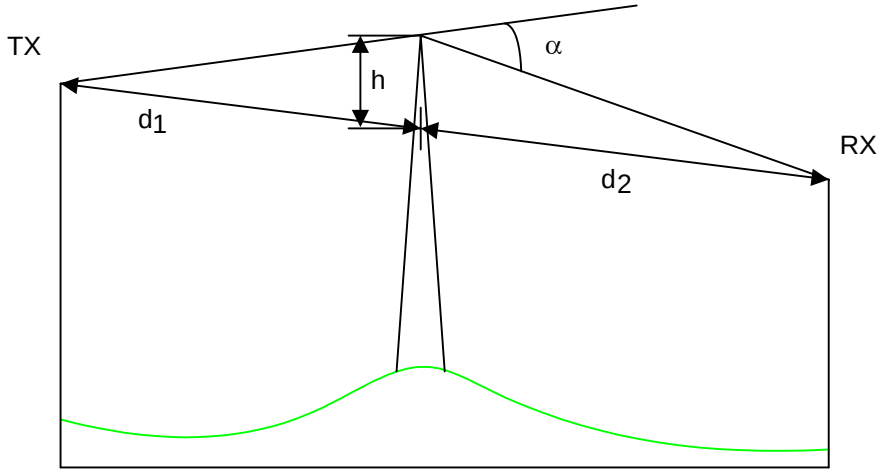

Figure 2.5 Knife-edge obstruction.

The diffraction gain in decibels due to the presence of a knife-edge is given as

$$G_d = 20 \log_{10} |F(\nu)| \tag{2.15}$$

Lee gives an approximate set of solutions for various values of ν [3].

Bullington proposed approximate techniques to compute diffraction losses over multiple knife-edges. The method by Bullington defines a new 'effective' obstacle at the point where the line-of-sight from the two antennas cross. A detailed description is given later in the chapter.

Epstein and Peterson also proposed techniques for approximating multiple knife-edge diffraction loses. Here they suggested drawing lines-of-sight between relevant obstacles and adding their respective diffraction loss [8].

2.3.3 Scattering

Scattering occurs when the radio path contains objects with dimensions that are small compared to the incident wavelength, and where the number of obstacles per unit volume is large. In a typical urban environment, lamp posts, street signs, foliage and rough surfaces scatter the transmitted radio signal in many directions, thereby providing RF coverage to locations which might not receive any signal via reflection or diffraction. Scattering, which follows the basic principles of diffraction is the most difficult to predict due to its random nature.

The roughness of a surface is often tested using the Rayleigh criterion [7], which defines a critical height h_c of surface protuberances for a given angle of incidence as given in Equation (2.16). A surface is considered smooth if its minimum to maximum protuberance is greater than h_c. For rough surfaces, the reflection coefficient needs to be modified by a scattering loss factor [3][7].

$$h_c = \frac{\lambda}{8 \cos \theta_i} \tag{2.16}$$

2.4 Propagation and k-factor

One of the most significant factors in the influence of radio wave propagation above 30 MHz is the large-scale variation of atmospheric refractive index with height, and the extent to which this changes with time. In practice, the measured median of the refractivity gradient in the first kilometer above ground in most temperate regions is about – 40 N-units/km [6]. Under the assumption of a constant refractivity gradient, the radio wave is an arc of circle of radius r, related to the refractive index n, by

$$1/r = -dn/d\,h_e \tag{2.17}$$

where h_e is the height above the Earth's surface in the same units as r. The effective Earth's radius a_e due to the change in refractive index is given by Equation (2.18), where a is the Earth's radius taken as 6.37×10^3 km.

$$1/a_e = 1/a - 1/r = 1/a + dn/d\,h_e \tag{2.18}$$

If the effective Earth's radius a_e is given by

$$a_e = ka \tag{2.19}$$

then $$k = a_e/a = 1/(1 + a\,dn/d\,h_e) = 1/\left[1 + a(dn/d\,h_e) \times 10^{-6}\right] \tag{2.20}$$

where k is the k-factor, or the effective earth-radius factor; $dn/d\,h_e$ is the gradient of the atmospheric refractive index with respect to height; $dN/d\,h_e$ is the gradient of refractivity per kilometer and is expressed as N-units/km. Since the refractive index of the troposphere is very nearly unity, the N-unit has been defined as $(n - 1) \times 10^6$.

When $dN/d\,h_e > -39$ N-units/km, the wave is said to be 'subrefracted' or bent down less than normal; that is, it is bent towards the sky ($0 < k < 4/3$).

When $dN/d\,h_e < -39$ N-units/km, the wave is said to be 'superrefracted' or bent down more than normal; in other words, the radio wave is bent towards the ground ($4/3 < k < \infty$).

When $dN/d\,h_e = -39$ N-units/km, it is said to be a $k = 4/3$ condition. Actually from a large number of experimental values obtained for the rate of refractivity with height, the average value has been found to be – 39 N-units/km. This standard value is

used to determine the normal refractive path of the radio beam through the atmosphere within 1 km of the Earth's surface.

The k-factor is an alternative and more often used method of describing the amount of bending undergone by a radio signal. Note during standard atmospheric conditions, the range of *k* is from 1.2 in dry elevated areas and 4/3 in typical inland areas, to 2 or 3 in humid coastal areas. If *k* equals infinity, the earth appears flat to the radio signal. If *k* becomes less than unity, the beam curves upwards away from the Earth's surface. This appears to the radio wave as if the Earth is 'bulging' and is going to obstruct the transmission path. This phenomenon is due to the atmospheric density increasing with height instead of decreasing with height. A subrefracting atmosphere is caused by the formation of fog created with the passage of warm air over a cool or moist surface. A superrefracting atmosphere results from conditions where there is a rise in temperature with increasing height or a marked decrease in total moisture content in the air with increasing height. An extreme case of superrefraction, that is negative *k*, will bend the radio wave downward with a radius smaller than that of the earth, and cause blackout fading if the receiver is beyond this point. Figure 2.6 illustrates the bending effects of differing k-factors on a radio beam.

In planning cellular radio systems, the k-factor is of great importance in the linking of base stations. Diffraction fading as described in Section 2.3.2 can be designed out of these systems by insuring that the antenna heights are sufficient, so that in the worst case of Earth bulge (k-factor minimum), the receiver antenna of one base station is not placed in the diffraction region.

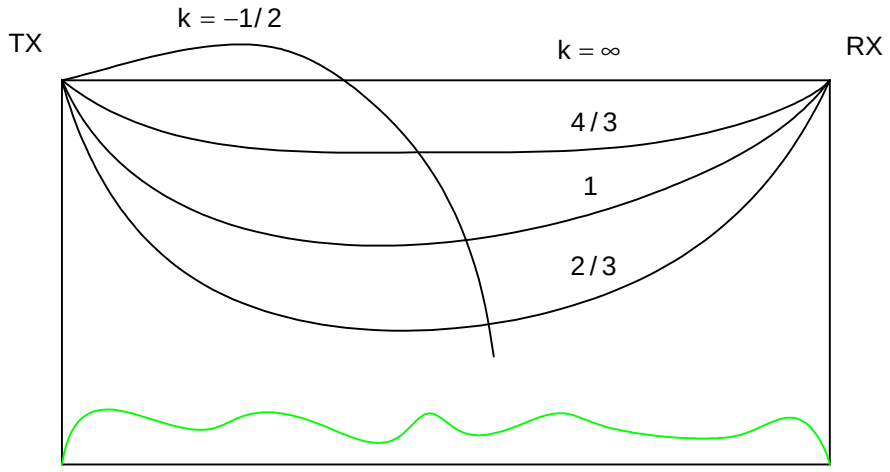

Figure 2.6 Variations of radio wave path for different k-factors.

2.5 Longley-Rice Model

A computer program has been published by Longley and Rice [9] that predicts the long-term median radio transmission losses over irregular terrain. The method predicts median values of attenuation relative to free space transmission loss and requires the following: the transmission frequency, the antenna separation, the height of the transmitting and receiving antennas, surface refractivity, the conductivity and dielectric constant of the Earth, polarization, and a description of the terrain. This program was based on thousands of measurements and compares well within the following ranges: frequency from 20 MHz to 40 GHz, antenna height between 0.5 to 3000 m, separation distance from1 to 2000 km and surface refractivity between 250 to 450 N-units.

The Longley-Rice method operates in two modes. When a detailed terrain path profile is available, predictions can be made using the point-to-point mode. On the other hand, if the terrain path profile is not available, the area mode prediction can be utilized. However this model is very meticulous when compared to other models and as such calculations can become rather lengthy.

2.6 Bullington Model

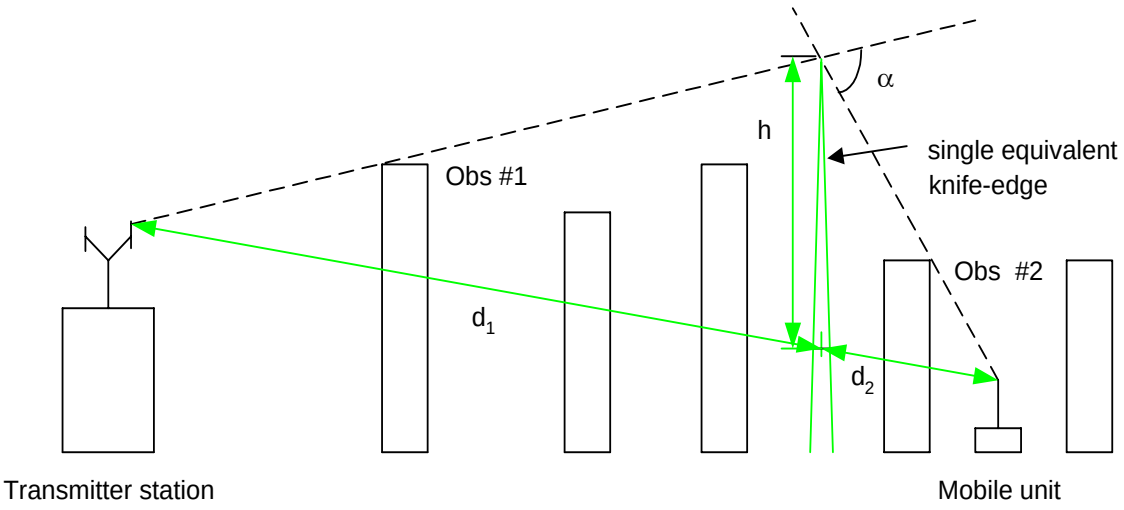

Figure 2.7 Bullington's approximation of obstructed path due to buildings.

Bullington in 1947, suggested that a single equivalent obstacle could replace a series of obstacles so that the path loss can be obtained using single knife-edge diffraction models [10]. This model however, oversimplifies the calculations and often provides

optimistic estimates of the received signal strength. Basically to estimate total path losses, calculated diffraction losses using the proposed technique is added to free space losses over the propagation path in question. To determine the actual diffraction parameter, Equation (2.14) is first applied. All parameters for satisfying this equation are obtained by geometrical solutions. Lee's diffraction gain approximations [3] in decibels for various obtained values of the diffraction parameter is given as

$$G_d = 0 \qquad \nu \le -1 \tag{2.21}$$

$$G_d = 20\log(0.5 - 0.62\nu) \qquad -1 \le \nu \le 0 \tag{2.22}$$

$$G_d = 20\log(0.5\exp(-0.95\nu)) \qquad 0 \le \nu \le 1 \tag{2.23}$$

$$G_d = 20\log\left(0.4 - \sqrt{0.1184 - (0.38 - 0.1\nu)^2}\right) \qquad 1 \le \nu \le 2.4 \tag{2.24}$$

$$G_d = 20\log\left(\frac{0.225}{\nu}\right) \qquad \nu > 2.4 \tag{2.25}$$

Referring to Equation (2.15), the diffraction gain expressions are in decibels, so for example when $\nu = 0$, the diffraction gain G_d is – 6dB.

Overall, this model has many practical applications in urban and rural areas.

2.7 Hata-Okumura Model

Okumura has laid down the groundwork for the Hata-Okumura model; his original model is indeed one widely used for signal prediction in urban areas. This model is applicable for frequencies in the range 150 – 2000 MHz and distances of 1 – 100 km. It also can be used for base station effective antenna heights ranging from 30 to 1000 m. Okumura developed a set of curves giving the median attenuation relative to free space, A_{mu}, in an urban area over a quasi-smooth terrain with a base station effective antenna height h_t of 200 m and a mobile antenna height h_m of 3 m. These curves were plotted as a function of frequency within the range of 100 – 3000 MHz and also as a function of distance from the base station in the range of 1 – 100 km [10]. Figure 2.8 illustrates typical urban propagation in a mobile environment.

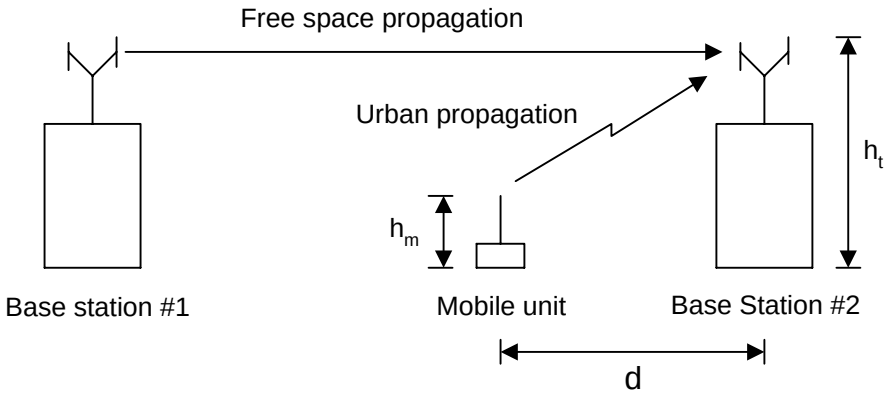

Figure 2.8 Typical urban propagation in a mobile environment.

To determine actual path loss using Okumura's model, the free space path loss between the points of interest is first determined, and then the value $A_{mu}(f,d)$, as read from the curves is added to it along with antenna height correction factors. This model is expressed as

$$PL = L_F + A_{mu}(f,d) + G(h_t) + G(h_m) \tag{2.26}$$

where PL is the median propagation loss in decibels, L_F the free space propagation loss, A_{mu} the median attenuation relative to free space, $G(h_t)$ the base station antenna height gain factor, and $G(h_m)$ the mobile antenna height gain factor.

However, the Okumura model is wholly based on measured data and does not provide any analytical explanations. In 1980, Hata [2] proposed a modified Okumura model that is now known as the Hata-Okumura model. This model is an empirical formulation of the graphical path loss information provided by Okumura. Here Hata presented the urban area propagation loss PL as a standard formula and supplied correction equations for other applicable situations. This standard formula is given as

$$\begin{aligned} PL = {} & 69.55 + 26.16 \log f - 13.82 \log h_t - a(h_m) \\ & + (44.9 - 6.55 \log h_t) \log d \end{aligned} \tag{2.27}$$

where loss is in decibels, f the transmitting frequency from 150 to 1500 MHz, h_t the

effective transmitter (base station) antenna height ranging from 30 to 200 m, h_m the effective mobile antenna height varying from 1 to 10 m, d is the transmitter-receiver separation distance in km, and $a(h_m)$ is the correction factor for effective mobile antenna height, which is a function of city size.

For a small to medium sized city, the correction factor is given by

$$a(h_m) = (1.1 \log f - 0.7)h_m - (1.56 \log f - 0.8) \tag{2.28}$$

and for a large city, it is given by

$$a(h_m) = 8.29(\log 1.54 h_m)^2 - 1.1 \qquad \text{for } f \leq 200 \text{ MHz} \tag{2.29}$$

$$a(h_m) = 3.2(\log 11.75 h_m)^2 - 4.97 \qquad \text{for } f \geq 400 \text{ MHz} \tag{2.30}$$

Note other correction factors exist for the suburban and open area [7].

Hata [3] further stated that since the propagation loss can be treated as a formula, it becomes possible to put the formula in to various calculations about system planning. However, since the formula can only be applied in restricted ranges, it is necessary to take notice of its applicable ranges and units. Using the following parameters: $f = 1500$ MHz, $h_t = 40$ m, $h_m = 1.5$ m, and assuming a midsize city, the path loss prediction for this model is shown graphically in Figure 2.9.

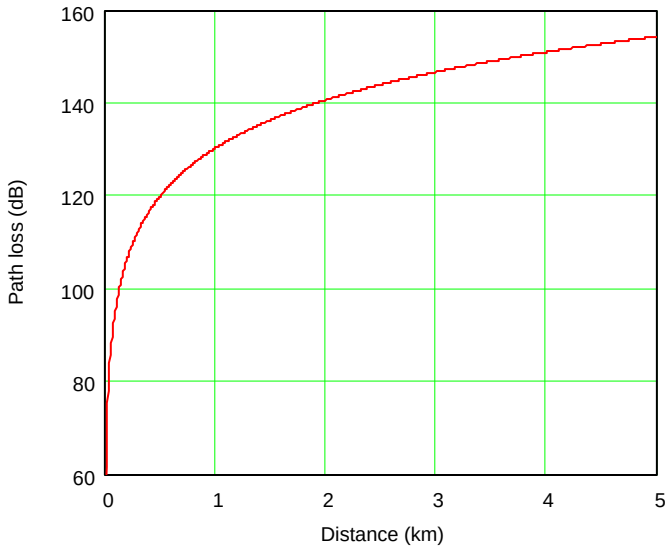

Figure 2.9 Hata-Okumura path loss prediction curve at 1500 MHz.

2.8 Walfisch-Ikegami Model

In this model for path loss prediction, over a frequency range of 800 – 2000 MHz, a distinction is made between line-of-sight and non-line-of-sight situations. It simulates the influence of buildings that take up the majority of urban land area. Here the elevated base station antenna is viewed as radiating fields that propagate over the roof tops by a process of multiple diffraction past rows of buildings that act as cylindrical obstacles [11]. Figure 2.10 illustrates the Walfisch-Ikegami propagation model. The model basically uses three equations: free space loss L_F, roof-to-street diffraction and scatter loss L_{rts}, and multi-screen loss L_{ms}. Here total path loss PL is given as Equation (2.31). The L_F equation is the standard free space model equation given in Equation (2.8). The L_{rts} equation

takes into consideration the width of the street W, the difference between shadowing building height and mobile unit height Δh_m, and L_0 a factor based on the incident angle ϕ relative to the street. The L_{rts} equation is given as Equation (2.32).

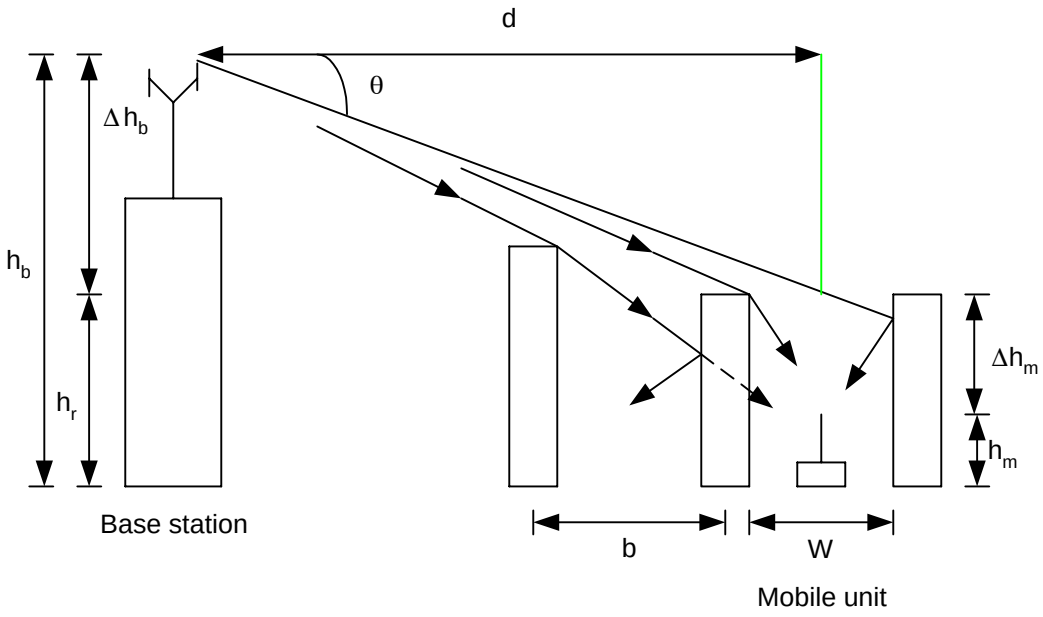

Figure 2.10 The Walfisch-Ikegami propagation model.

$$PL = L_F + L_{rts} + L_{ms} \tag{2.31}$$

$$L_{rts} = 20 \log \Delta h_m - 10 \log W + 10 \log f + L_0 - 16.9 \tag{2.32}$$

where $$L_0 = 4 - 0.114(\phi - 55) \quad (2.33)$$

assuming ϕ to be 90^o.

The L_{ms} equation considers basically the distance between buildings b, and other correction factors. This equation is given as

$$L_{ms} = L_{bsh} + k_a + k_d \log d + k_f \log f - 9 \log b \quad (2.34)$$

where $$L_{bsh} = -18 \log 11 + \Delta h_b \text{ for } h_b > h_r \qquad \text{for } h_b > h_r \quad (2.35)$$

$$k_a = 54 \qquad \text{for } h_b > h_r \quad (2.36)$$

$$k_d = 18 - \frac{15 \Delta h_b}{\Delta h_m} \qquad \text{for } h_b \geq h_r \quad (2.37)$$

$$k_f = 4 + 0.7\left(\frac{f}{925} - 1\right) \qquad \text{for midsize city} \quad (2.38)$$

The Walfisch-Ikegami model is a very practical propagation model. However, it is only applicable for base station heights ranging from 4 – 50 m, mobile unit antenna heights between 1 – 3 m, and distances of 0.02 – 5 km.

Figure 2.11 shows a comparison of the path loss predicted by the Hata-Okumura and Walfisch-Ikegami models using the following data: $f = 2400$ MHz, $h_m = 1.5$ m, $h_b = h_t = 40$ m, $h_r = 15$ m, $b = 30$ m, $W = 15$ m, $\phi = 90^o$, and assuming flat roofs.

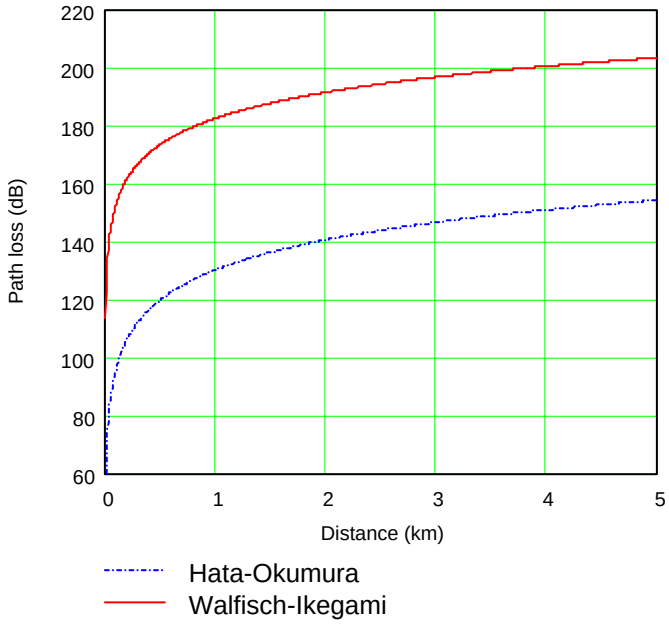

Figure 2.11 Path loss comparison between the Hata-Okumura and Walfisch-Ikegami models.

The path losses predicted by the Hata-Okumura model are approximately 40 dB lower than those predicted by the Walfisch-Ikegami model. This is somewhat expected since the Hata-Okumura model ignores effects from buildings and streets.

CHAPTER 3

SPREAD SPECTRUM COMMUNICATIONS

Since the late 1940s, spread spectrum communication techniques have been applied to a variety of electronic systems and applications. Today these techniques are widely used in digital cellular radios, wireless local area networks (WLANs), personal communication networks (PCNs), traffic control systems, and the global positioning system (GPS), to name a few. In 1983, the US Federal Communication Commission (FCC) allotted three new frequency bands, 902-928 MHz, 2400-2483.5 MHz and 5725-5850 MHz, to commercial spread spectrum users. Interestingly with spread spectrum technology, the total user capacity of any of these assigned frequency bands may be larger than is possible by other conventional methods, such as Frequency Division Multiple Access (FDMA) or Time Division Multiple Access (TDMA).

3.1 Fundamentals of Spread Spectrum

A system is defined to be a spread spectrum system if it fulfills the following requirements: (i) the signal occupies a bandwidth much in excess of the minimum bandwidth necessary to send the information, (ii) spreading is accomplished by means of

a spreading signal, often called a code signal, which is independent of the data, and (iii) at the receiver, despreading (recovering the original data) is accomplished by the correlation of the received spread signal with a synchronized replica of the spreading signal used to spread the information [13]. Note however, modulation schemes such as frequency modulation and pulse code modulation also spread the spectrum of an information signal, but they do not qualify as spread spectrum systems since they do not satisfy all the conditions outlined before.

Spread spectrum techniques can be very useful in solving a wide range of communication problems. The amount of performance improvement that is achieved through the use of spread spectrum is defined as the processing gain of the spread spectrum system. That is, processing gain is the difference between system performance using spread spectrum techniques and system performance not using spread spectrum techniques, all else being equal. One approximation often used for processing gain is the ratio of the spread bandwidth to the information rate.

Let us now consider sending a message using a transmitted power S Watts (W) at an information rate R_b bits/s (bps). By introducing a spread spectrum (SS) modulation, the bandwidth of the transmitted signal is increased from R_b Hz to W_{ss} Hz where $W_{ss} >> R_b$ denotes the spread spectrum bandwidth. Assume that the channel introduces, in addition to the usual thermal noise N_0 W/Hz (single-sided power spectral density), an additive interference (jamming) having power J distributed over some bandwidth W_J. After despreading, the desired signal bandwidth is once again equal to R_b Hz and the

interference power spectral density (PSD) is now $N_J = J/W_{ss}$. Note that since the thermal noise is assumed to be white; that is, it is uniformly distributed over all frequencies, its PSD is unchanged by the despreading operation and, thus, remains equal to N_0. Regardless of the signal and jammer waveforms, the equivalent bit energy-to-total noise ratio is, in terms of the given parameters,

$$\frac{E_b}{N_t} = \frac{E_b}{N_0 + N_J} = \frac{S/R_b}{N_0 + J/W_{ss}} \tag{3.1}$$

For most practical scenarios, the jammer limits performance and, thus, the effects of receiver noise in the channel can be ignored. Therefore assuming $N_J >> N_0$, we can rewrite Equation (3.1) as

$$\frac{E_b}{N_t} \cong \frac{E_b}{N_J} = \frac{S/R_b}{J/W_{ss}} = \frac{S}{J} \cdot \frac{W_{ss}}{R_b} \tag{3.2}$$

where the ratio J/S is the jammer-to-signal power ratio and the ratio W_{ss}/R_b is the spreading ratio and is defined as the processing gain of the system. Equation (3.3) therefore gives the processing gain as

$$G_p = \frac{W_{ss}}{R_b} \tag{3.3}$$

Note for direct sequence systems, W_{ss} is approximately the code chip rate R_c and R_b is similarly the information bit rate. In this case, the processing gain is expressed as

$$G_p = \frac{R_c}{R_b} \tag{3.4}$$

Since the bit error probability of the communications receiver depends on the ratio E_b/N_J, we can see that by minimizing J/S (by choice of S) and maximizing G_p (by choice of W_{ss} or R_c, for a given desired information bit rate) its performance will be greatly improved.

3.2 Spreading Techniques

There are primarily two spread spectrum techniques, direct sequence spread spectrum, an amplitude modulation technique and frequency hopping spread spectrum, a frequency modulated technique. The goal of both of these techniques is to take the power to be transmitted and spread it over a very wide bandwidth so that the power per unit bandwidth (W/Hz) is minimized. When this is achieved, the transmitted spread spectrum power received by any existing user, having a relatively narrow bandwidth, is only a fraction of the actual transmitted power. Lets take a simple case for example, if a transmitted signal having a power of 1 W is spread over a bandwidth of 100 MHz and an existing user employs a communication system (say a mobile radio) having a bandwidth

of 1 MHz, then the effective interference power in the narrow band communication system is reduced by a factor of 100, and is 1 W divided by 100, or 10 mW.

The feature of spread spectrum that results in interference reduction is that the spread spectrum receiver actually spreads the received energy of any potential jammer over the same wide bandwidth (100 MHz as in example), while compressing the bandwidth of the desired received signal back to its original bandwidth.

Note that for the spread spectrum system to operate properly, it is necessary for the receiver to acquire the correct phase position of the incoming signal waveform, and it must continually track that phase position so that loss of lock will not occur. The two processes of acquisition and tracking outlined in Sklar [13], form the synchronization subsystem of a spread spectrum receiver. Signal acquisition is typically accomplished by a search of as many phase positions as necessary until one is found which results in a large correlation between the phase of the incoming signal and the phase of the locally generated spreading sequence at the receiver. Tracking is more often performed with a delay-locked-loop (DLL). The importance of the combined synchronization process cannot be overstated; for if synchronization is not both achieved and maintained the desired signal cannot be despread.

3.2.1 Direct Sequence Spread Spectrum

Direct sequence (DS) spread spectrum systems employ a spreading code, along with the information or data signal to modulate their RF carrier. Here the chip rate of the spreading code is typically much larger than the bit rate of the data signal. The spreading

code or wide band signal, is chosen to have two possible amplitudes, + 1 and – 1. These amplitudes are usually sequentially switched, in a pseudorandom manner, periodically. The theory behind the various spreading codes used in the actual spreading operation is presented a little later in this chapter. Figure 3.1 illustrates a simple model of a DS spread spectrum modulator.

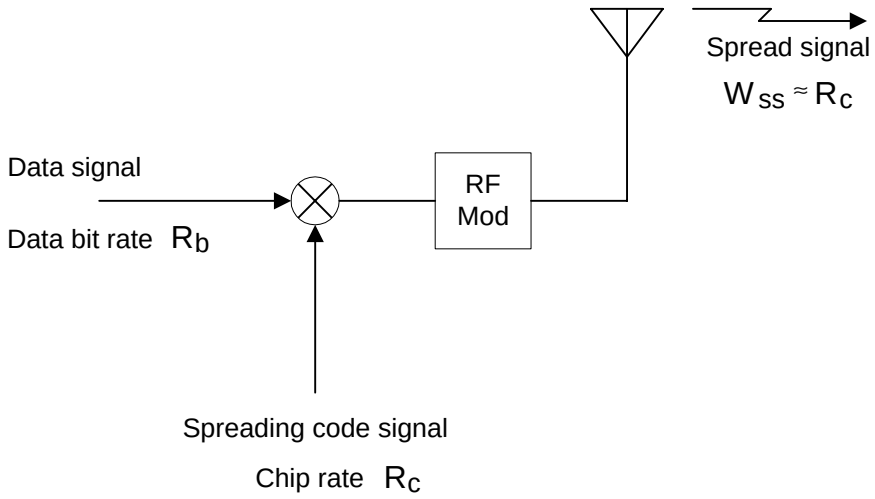

Figure 3.1 DS spread spectrum modulator.

Various modulation techniques are used in DS spread spectrum systems such as binary phase shift keying (BPSK), quadrature phase shift keying (QPSK) and minimum shift keying (MSK) to name a few [5]. The simplest form of DS spread spectrum however, employs the BPSK technique.

3.2.1.1 DS/BPSK Spread Spectrum

Sklar [13] gives the general expression for a phase shift keying (PSK) waveform as

$$s_i(t) = \sqrt{\frac{2E}{T}} \cos\left[\omega_0 t + \phi_i(t)\right] \qquad 0 \le t \le T\ ;\ i = 1.....M \tag{3.5}$$

where the phase term $\phi_i(t)$ will have M discrete values, typically given by

$$\phi_i(t) = \frac{2\pi i}{M} \qquad i = 1.....M \tag{3.6}$$

In the single case of BPSK however, M takes on a value of 2. The parameter E is symbol energy, T is symbol time duration, and $0 \le t \le T$. Basically in BPSK modulation the modulating data signal shifts the phase of the waveform $s_i(t)$, to one of two states either 0 or π (180^o). This can be mathematically represented as a multiplication of the carrier by a function $c(t)$, which takes on the values ± 1. Figure 3.2 shows a simulated BPSK waveform for a 13-bit Barker code pseudorandom (PN) sequence.

Lets consider a constant-envelope data-modulated carrier having power P, where $P = E/T$, radian frequency ω_0, and data phase modulation $\theta_d(t)$, as defined by Equation (3.7) overleaf.

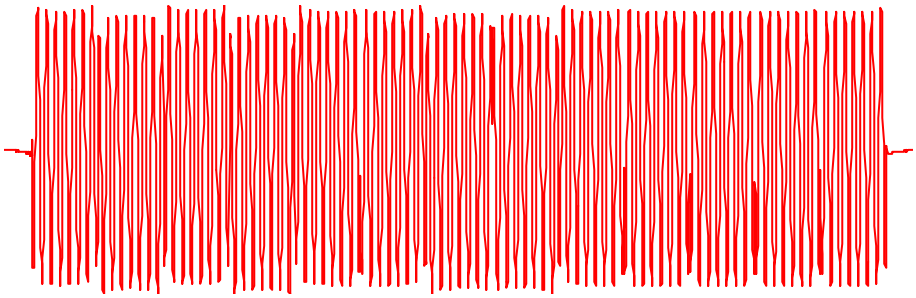

(a) 13-bit Barker code PN sequence

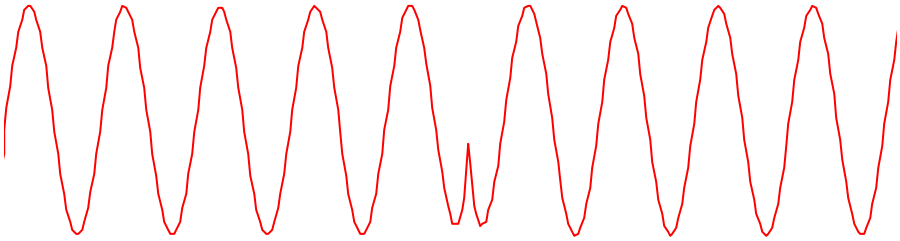

(b) Magnified view of part of waveform

Figure 3.2 BPSK simulated waveform for a 13-bit Barker code PN sequence.

$$s_d(t) = \sqrt{2P}\cos[\omega_0 t + \theta_d(t)] \tag{3.7}$$

This signal occupies a bandwidth typically between one-half and twice the data rate prior to DS spreading, depending on the details of the data modulation [5]. BPSK spreading is therefore accomplished by multiplying $s_d(t)$ by the function $c(t)$ representing the spreading waveform as illustrated in Figure 3.3. The transmitted signal is now given as

$$s_t(t) = \sqrt{2P}c(t)\cos[\omega_0 t + \theta_d(t)] \tag{3.8}$$

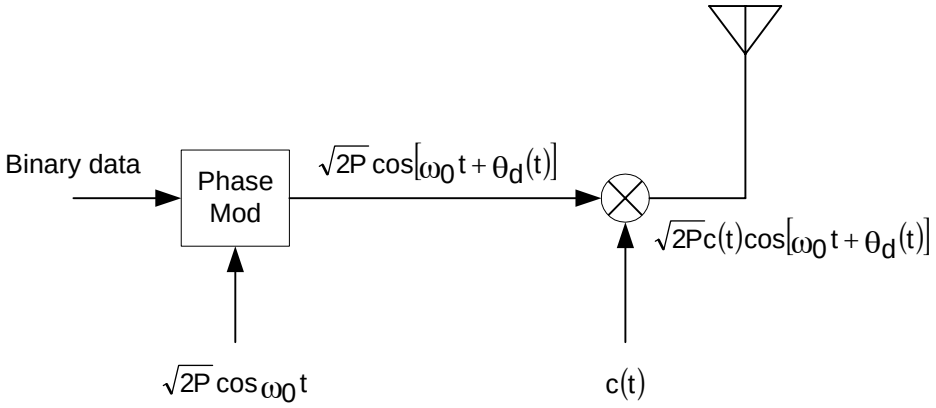

Figure 3.3 DS/BPSK spread spectrum transmitter.

If the signal is transmitted via a typical channel having a transmission delay T_d, the signal will be received together with some type of interference and/or Gaussian noise. Demodulation is accomplished by remodulating the received signal with a synchronized replica of the spreading code $c(t - T_{d'})$, here appropriately delayed as illustrated in Figure 3.4. This remodulation or correlation of the received signal with the delayed spreading waveform is called despreading, and is a critical function in all spread spectrum systems. The output signal component after the despreading operation is given as Equation (3.9), where $T_{d'}$ is the receiver's best estimate of the transmission delay. Since $c(t) = \pm 1$, the product $c(t - T_d) \times c(t - T_{d'})$ will be unity if $T_{d'} = T_d$, that is, if

the spreading code at the receiver is synchronized with the spreading code at the transmitter. When correctly synchronized the signal component at the output of the receiver's despreading mixer is equal to $s_d(t)$ except for a random phase ϕ, and $s_d(t)$ can be modulated using a conventional coherent phase demodulator.

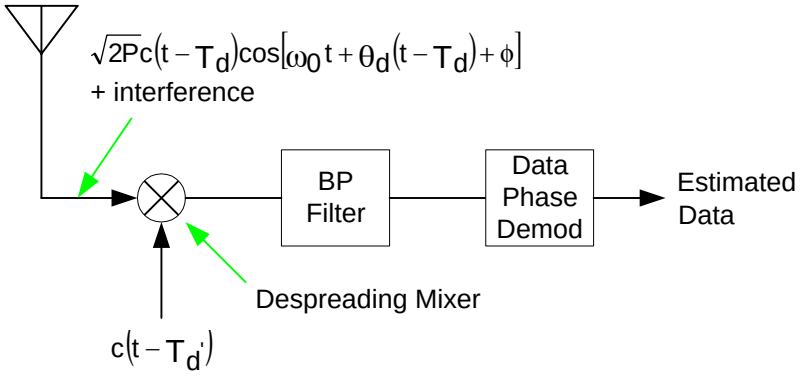

Figure 3.4 DS/BPSK spread spectrum receiver.

$$\sqrt{2P}c(t-T_d)c(t-T_{d'})\cos[\omega_0 t+\theta_d(t-T_d)+\phi] \tag{3.9}$$

As indicated in the above derivations the data modulation does not have to be BPSK. However, if BPSK is used as the digital phase modulation for the data, $\theta_d(t)$ can be ignored based on Equation (3.6). The data signal will then take on values of ± 1 resulting in Equation (3.8) becoming simply Equation (3.10), where $d(t)$ represents the data signal.

$$s_t(t) = \sqrt{2P}c(t)d(t)\cos\omega_0 t \tag{3.10}$$

3.2.2 Frequency Hopping Spread Spectrum

In a frequency hopping (FH) system, like the DS system, a wide band frequency spectrum is desired. This is achieved by allowing its carrier frequency to "hop" from frequency to frequency over a wide band of frequencies. The specific order in which frequencies are occupied is a function of a code sequence, and the rate of hopping from one frequency to another is a function of the data rate.

The transmitted (power) spectrum of a FH signal is quite different from that of a DS system. Instead of a sampling function squared-shaped envelope, the power spectrum of the FH signal is flat over the band of frequencies used. Therefore, the bandwidth of a FH signal is simply w times the number of frequency slots available, where w is the bandwidth of each hop channel.

To fully understand FH spread spectrum, lets say an entire allocated bandwidth is 1,000 times wider than the bandwidth of a transmitted signal, then during a given time interval this signal can be transmitted at any one of a 1,000 possible frequencies. The result is reduced interference to any existing user. For example, if an existing narrow band user occupies one of the 1,000 frequency slots, then interference with the existing user occurs only 1/1000 of the total time. During the remaining time, the transmission has hopped to different frequencies, and therefore does not cause interference.

FH systems can be either of the fast frequency hopping (FFH) type or the slow frequency hopping (SFH) type [5][13]. In the FFH system, the frequency hopping occurs

at a rate that is greater than the information or data rate. In the SFH system, the hop rate is less than the data rate. There is, of course, an intermediate situation in which the hop rate and data bit rate are of the same order of magnitude.

Generally, FH systems experience occasional burst errors, while DS systems experience continuous but lower-level random errors. With DS systems, single errors are dispersed randomly over time; with FH systems, errors are distributed in clusters resulting in the need for error correction codes. Burst errors are attributable to fading or single-frequency interference, which is time and frequency dependent. The typical DS system however, spreads the data in both the time and frequency domains, thus providing time and frequency diversity and minimizing the effects of fading and interference. On an overall basis the primary trade-off in DS and FH systems [4] are presented in Table 3.1, it is very clear at this point that design standards play a key role in the choice of a suitable spread spectrum system.

Table 3.1 Primary trade-off in DS and FH systems.

DIRECT SEQUENCE	FREQUENCY HOPPING
Good range resolution	Poor range resolution
More noise-like signal	Narrow instantaneous bandwidth
Can operate without error correction codes	Requires error correction codes due to burst errors in noisy frequency slot
Limited near-far performance	Best near-far performance
Requires linear signal path	Operates well with non-linearity in signal path
Synchronization more difficult	Easier to synchronize

3.3 Code Division Multiple Access

As is well known, the two most common multiple access techniques are frequency division multiple access (FDMA) and time division multiple access (TDMA). In FDMA, all users transmit simultaneously, but use disjoint frequency bands. In TDMA, all users occupy the same RF bandwidth, but transmit sequentially in time. When users are allowed to transmit simultaneously in time and occupy the same RF bandwidth as well, some other means of separating the signals at the receiver must be available, and code division multiple access (CDMA) provides this necessary capability. At this point CDMA can be considered as a hybrid of FDMA and TDMA.

CDMA is a DS or FH spread spectrum system in which a number (two or more) of spread spectrum signals communicate simultaneously, each operating over the same frequency band. In a CDMA system, each user is given a distinct sequence. This sequence identifies the user. For example, if user 1 has a sequence S_1, user 2 a sequence S_2, etc., then a receiver, desiring to listen to user 1 will receive at its antenna all of the energy sent by all of the users. However, after despreading user 1's signal, it will see all the energy of user 1 but only a small fraction of the energies sent by users 2 and 3, for example.

CDMA is interference limited; that is, the number of users that can use the same spectrum and still have acceptable performance is determined by the total interference power that all of the users, taken as a whole, generate in the receiver. Unless one takes great care in power control, those CDMA transmitters that are close to the receiver will cause the overwhelming interference. This effect is known as the "near-far" problem. In a

mobile environment, the near-far problem could be the dominant effect. Fortunately, it is possible to control the power of each mobile user so that the received power from each mobile user is the same. This technique is called “adaptive power control”.

3.4 Pseudorandom Sequences

In CDMA systems, pseudorandom noise (PN) sequences are used to perform the following tasks [13]:

- Spread the bandwidth of the modulated signal to the larger transmission bandwidth.
- Distinguish among the different user signals by using the same transmission bandwidth in the multiple-access scheme.

PN sequences are not literally random as the word pseudorandom implies, they are deterministic periodic sequences; however, to an authorized listener in a spread spectrum system they appear to be truly random. Hence, the PN sequence is defined based on randomness properties. Garg, Smolik and Wilkes [12] give three key properties of an ideal PN sequence as follows:

- The relative frequencies of zero and one are each 1/2.
- For zeros or ones, half of all run lengths are of length 1; one quarter of length 2; one eighth are of length 3; and so on.
- If a PN sequence is shifted by any nonzero number of elements, the resulting sequence will have an equal number of agreements and disagreements with respect to the original sequence.

While they are many PN sequences such as the maximal length sequence, Gold, Barker and, Kassami sequences, of all the most commonly used is the maximal length sequence [5][14].

3.4.1 Maximal Length Sequences

Maximal length sequences (m-sequences) are PN sequences that cycle with a period $2^n - 1$, where n is an integer. Primitive polynomials are used to generate these sequences, which are then implemented using linear feedback shift registers (LFSRs), and exclusive-OR gates. M-sequences possess good randomness properties including a two-valued autocorrelation function [5].

3.5 Fading in CDMA Channels

The concept of fading in CDMA channels is an important one in fully understanding the design and performance of digital cellular communication systems. Depending on the relation between signal parameters (such as bandwidth and symbol period) and channel parameters (such as delay spread and Doppler spread) different transmitted signals will undergo different types of fading. The time dispersion and frequency dispersion mechanisms in a mobile channel lead to four possible distinct effects, which are manifested depending on the nature of the transmitted signal, the channel, and the velocity [3]. Multipath delay spread leads to flat fading and frequency selective fading. Doppler spread leads to fast fading and slow fading. The two propagation mechanisms are independent of each other.

3.5.1 Multipath Delay Spread

Delay spread is a parameter, which describes the dispersal nature of the channel in a local area. It does not provide information about the time varying nature of the channel caused by either relative motion between mobile unit and base station, or by movement of objects in the channel. The time dispersal properties of CDMA multipath channels are most commonly quantified by their mean excess delay and rms delay spread as given in Rappaport [3]. In general, time dispersion due to multipath causes the transmitted signal to undergo either flat fading or frequency selective fading. Both of which are of great concern to digital communication system designers.

3.5.1.1 Flat Fading

Rappaport [3] states if the mobile radio channel has a constant gain and linear phase response over a bandwidth that is greater than the bandwidth of the transmitted signal, then the received signal will undergo flat fading. In flat fading, the multipath structure of the channel is such that the spectral characteristics of the transmitted signal are preserved at the receiver. However, the strength of the received signal varies with time, due to fluctuations in the gain of the channel caused by multipath. Thus, changes in channel gain result in changes of amplitude in the received signal. Typical flat fading channels cause deep fades or outage time, and therefore may require 20 or 30 dB more transmitter power to achieve low BERs during times of deep fades compared to systems operating over non-fading channels. One significant parameter for evaluating the quality of a digital cellular communication system is the outage time, or the probability of

exceeding a stated BER. To summarize, a transmitted signal undergoes flat fading if its bandwidth is much less than the channel bandwidth, or if the rms delay spread, is much less than its symbol period or duration.

3.5.1.2 Frequency Selective Fading

Rappaport [3] states if a channel possesses a constant-gain and linear phase response over a bandwidth that is smaller than the bandwidth of the transmitted signal, then the channel creates frequency selective fading on the received signal. Under such conditions, the channel impulse response has a multipath delay spread which is greater than the reciprocal bandwidth of the transmitted message waveform. When this occurs, the received signal includes multiple versions of the transmitted waveform which are attenuated (faded) and delayed in time, and hence the signal is distorted. Frequency selective fading is due to time dispersion of the transmitted symbols within the channel. Thus, the channel induces intersymbol interference (ISI). To summarize, a transmitted signal undergoes frequency selective fading if its bandwidth is much greater than the channel bandwidth; or if the rms delay spread, is much greater than its symbol period or duration.

3.5.2 Doppler Spread

Doppler spread is a measure of the spectral broadening caused by the time rate of change of the mobile radio channel, and is defined as the range of frequencies over which the received Doppler spectrum is essentially zero [3]. Lets consider a case where a single

component of frequency f_c is transmitted, the received signal spectrum will have new components $f_c - f_d$ to $f_c + f_d$ where f_d is the Doppler shift. The amount of spectral broadening depends on f_d which is a function of the relative velocity of the mobile unit, the angle θ between the direction of motion of the mobile unit and direction of arrival of the scattered waves, and λ the wavelength of the transmitted signal. Doppler shift can be defined as

$$f_d = \frac{v}{\lambda} \cdot \cos\theta \tag{3.11}$$

where v is the constant velocity of the mobile unit; assuming communications are between mobile unit and base station.

Coherence time T_c is the time domain dual of Doppler spread f_m, and is used to characterize the time varying nature of the frequency dispersal of the channel in the time domain [3]. Coherence time can be defined as

$$T_c \approx \frac{1}{f_m} \tag{3.12}$$

Depending on how rapidly the transmitted signal changes as compared to the rate of change of the channel determines whether a channel can be classified as either of the fast fading or slow fading type.

3.5.2.1 Fast Fading

In a fast fading channel, the channel impulse response changes rapidly within the symbol duration [3]. That is the coherence time of the channel is smaller than the symbol period of the transmitted signal. This causes frequency dispersion (also called time selective fading) due to Doppler spreading, which leads to signal distortion. In practice, fast fading only occurs for very low data rates. Therefore, a signal undergoes fast fading if its symbol period is greater than the coherence time, and its transmitted bandwidth is less than the Doppler spread.

3.5.2.2 Slow Fading

In a slow fading channel, the channel impulse response changes at a rate much slower than the transmitted signal [3]. In this case, the channel may be assumed static over one or several reciprocal bandwidth intervals in the frequency domain, this implies that the Doppler spread of the channel is less than the bandwidth of the transmitted signal. Therefore, a signal undergoes slow fading if its symbol period is much less than the coherence time, and its transmitted bandwidth is much greater than the Doppler spread.

3.6 Rayleigh and Ricean Fading Models

In mobile radio channel, the Rayleigh fading distribution [3] is commonly used to describe the statistical time varying nature of the received envelope of a flat fading signal. This model has widespread applications in simulating mobile unit to base station

communications. On the other hand, in mobile to mobile communications the Ricean fading model [3] finds most applications. The effect of a dominant signal arriving with many weaker multipath signals gives rise to the Ricean fading distribution.

3.7 Channel Improvement Techniques

Mobile communication systems require signal-processing techniques that improve the link performance in hostile mobile radio environments. Equalization, diversity and channel coding are proven channel improvement techniques. These techniques minimize the probability of error, which greatly determines the choice of the threshold level.

3.7.1 Equalization

Intersymbol interference (ISI) caused by multipath in frequency selective time dispersal channels distorts the transmitted signal, causing bit errors at the receiver. ISI has been recognized as the major impediment to high-speed data transmission over mobile radio channels. Equalization is a technique used to combat ISI. In mobile radio channels, a variety of adaptive equalizers can be used to cancel interference while providing diversity. Since the mobile fading channel is truly random and time varying, equalizers must track the time varying characteristics of the mobile channel, and thus are called adaptive equalizers. An adaptive equalizer is normally implemented at baseband, called time domain equalization, or at the intermediate frequency (IF) stage in the receiver, called frequency domain equalization [3][6][13]. Adaptive equalization can perform well if the channel error performance is satisfactory and not poor.

3.7.2 Diversity

Diversity is a commonly used technique in mobile radio systems to combat signal fading. In explaining diversity lets say several replicas of a baseband signal are received over multiple channels with comparable strengths and exhibiting independent fading, then there is a good likelihood that at least one or more of these received signals will not fade at any given instant in time. This makes it possible to deliver an adequate signal level to the receiver. In mobile radio, the power available on the reverse link is severely limited by the battery capacity in hand held units. Diversity methods therefore play a crucial role in reducing transmit power needs, a factor well limited in spread spectrum communications. There are many diversity methods such as space, polarization, angle, frequency, path and time [3][6][7]. However, the most popularly used methods are that of space, frequency and path.

3.7.2.1 Space Diversity

In space diversity, spatially spaced antennas are used at either the base station or mobile unit. By using base station antennas that are sufficiently separated in space, the base station is able to improve the reverse link by selecting the antenna with the strongest signal from the mobile unit. The spacing of the antennas in the receiving or transmitting array is chosen so that the individual signals received are uncorrelated. In practice, it is not possible to achieve zero correlation (uncorrelated signals), or even a very low value, but fortunately substantial benefits are obtained. Space diversity can be used in both the horizontal and vertical planes.

3.7.2.2 Frequency Diversity

Frequency diversity can be defined as the simultaneous transmission of the same signal over two or more radio frequency channels that are located in the same band. The frequency separation between carriers should be larger than the coherence bandwidth. This technique has the disadvantage that it not only requires spare bandwidth but also requires that there be as many receivers as there are channels used for the frequency diversity.

3.7.2.3 Path Diversity

This method finds application in DS CDMA spread spectrum. Based on theory, spread spectrum signals can resolve multipath arrivals as long as the path delays are separated by at least one chip period. If a signal in each path shows low-fade correlation, as is usually the case in frequency selective fading, these paths offer a valuable source of diversity. A receiver that resolves multipath via correlation and then combines them is referred to as a Rake receiver [3][13].

3.7.3 Channel Coding

Channel coding protects digital data from errors by selectively introducing redundancies in the transmitted data. Channel codes that are used to detect errors are called error detection codes, while codes that can detect and correct errors are called error correction codes.

CHAPTER 4

MATHCAD MODEL

The Mathcad model is the development of a computerized signal propagation and coverage prediction system. Mathcad 7.0 software is used here to generate path loss (PL) contour plots and various bit error rate (BER) plots. This software program is a worldwide standard for technical calculations both at the student and professional level.

The first step in developing this model was to establish a simple base program called PLsim. This base program was used to run simulated terrain data for various existing propagation models presented in Chapter 2.

4.1 PLsim Program

In Mathcad, a contour plot is executed using an input data matrix. A matrix is a rectangular array of numbers. A single element in a matrix M is defined as $M_{i,j}$, where i specifies the ith row and j the jth column the element occupies. Both i and j must be dimensionless integers. Note at this point, Mathcad starts all arrays at zero by default.

To convert path loss data into a matrix format, the propagation coverage area is first viewed as a XY coordinate system. If we consider a transmitter as being located at

the origin, then any position relative to this point whether occupied by a receiver or an obstruction can be defined in terms of x and y coordinates. For example, say a 5×5 km square map represents a propagation coverage area. For a 1 km grid resolution, x will take on a range of values such that $x = -5,-4.....5$ and similarly y such that $y = -5,-4.....5$. If obstructions are positioned at points (1, 4), (0, 4), (-2, 3) and (4, -2) respectively, then a mapped layout of the coverage area will be as shown in Figure 4.1.

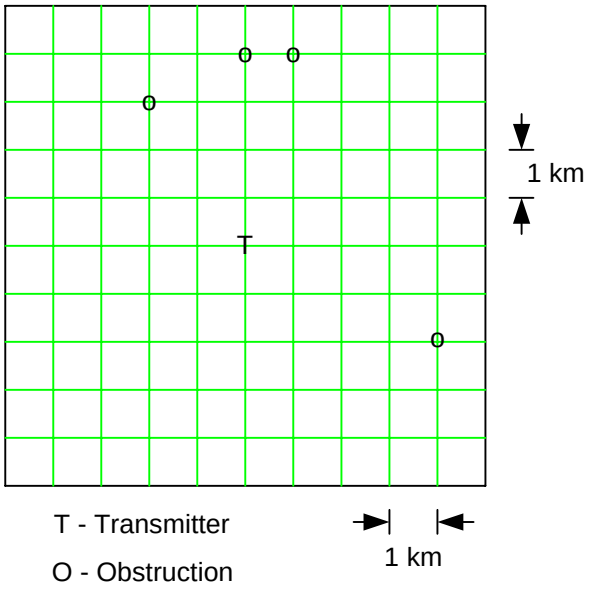

Figure 4.1 Mapped layout of propagation coverage area.

Based on the Cartesian coordinate system, the distance between the designated transmitted position (0, 0) and any relative point on the mapped layout can be calculated

using Equation (4.1), where d represents distance in km. At this point in the PLsim program, a practical assumption is made that all distances are small with respect to the curvature of the Earth.

$$d = \sqrt{x^2 + y^2} \tag{4.1}$$

The second stage of the PLsim program converts x and y coordinates of the mapped layout into a matrix grid. To do this operation a simple Mathcad program is used as shown in Figure 4.2.

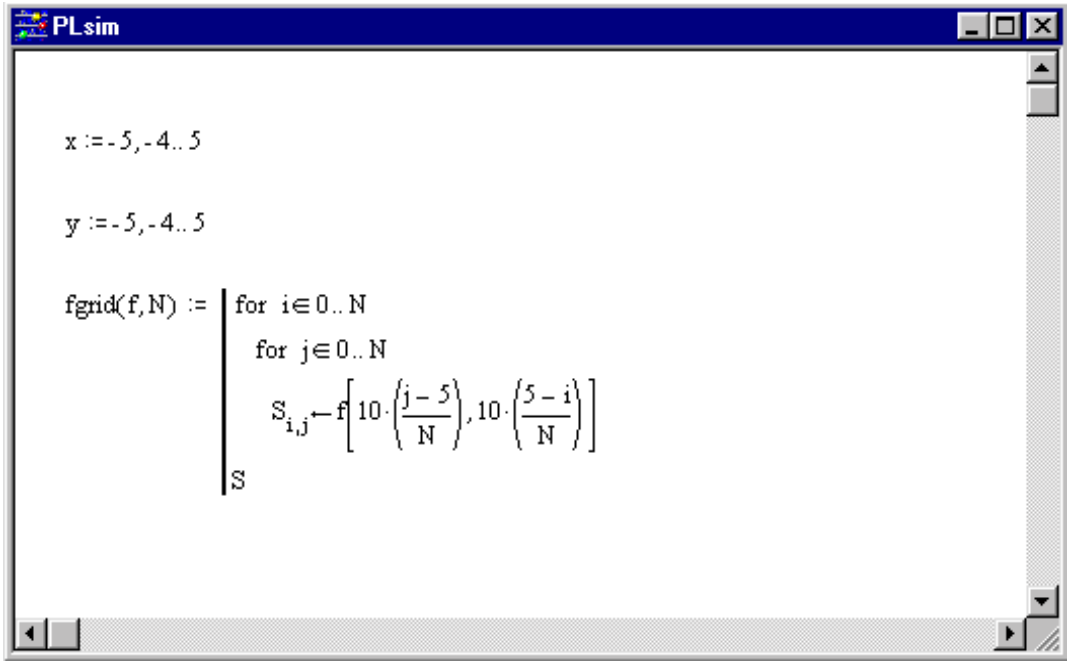

Figure 4.2 Mathcad conversion program.

The function $fgrid(f, N)$ takes a function of two variables f as an argument and an integer N and returns a $(N+1)\times(N+1)$ grid of values of f over the square. Therefore, since a path loss equation is defined in terms of d, it is a function of x and y, and subsequently can be applied.

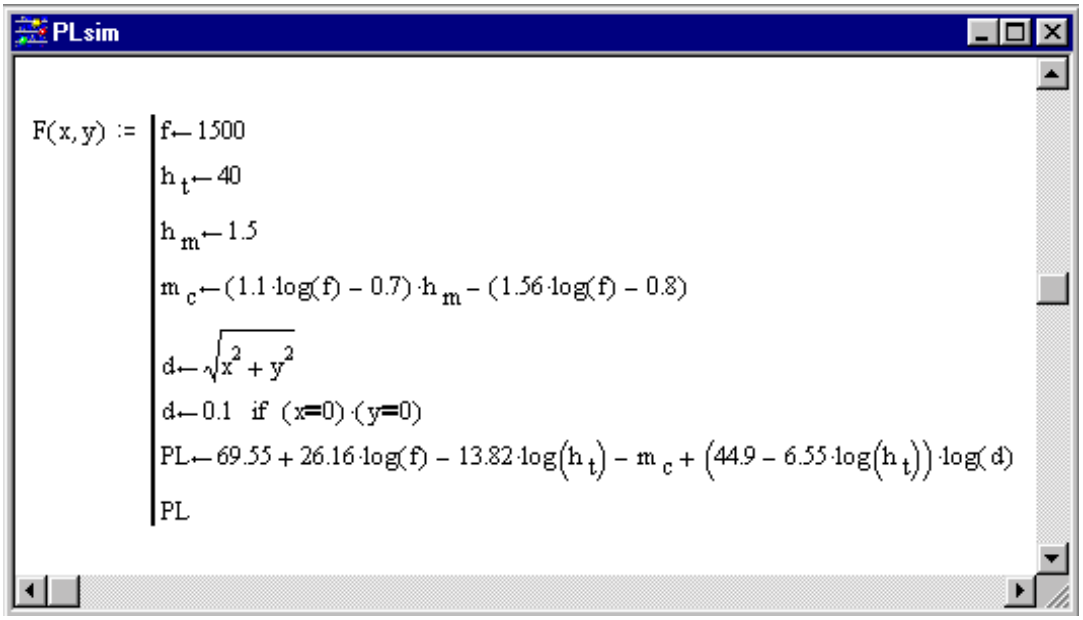

Figure 4.3 Standard formula for Hata-Okumura model as a function of x and y.

4.1.1 Hata-Okumura Model Simulation

In order to simulate path loss, a Mathcad program is devised that returns the standard formula used for this model as a function of x and y. This standard formula was presented in Chapter 2, as Equation (2.27). The parameters used here are the same as

those used for the graphical illustration in Figure 2.9. This program is defined by $F(x,y)$ as shown in Figure 4.3. Note the correction factor for effective mobile antenna height $a(h_m)$ is expressed here as m_c.

After the program is executed, an 11×11 matrix M is returned as shown in Figure 4.4. However, since the Hata-Okumura model ignores the effects of buildings and streets, a few building obstructions are created. These simulated buildings each represent an assumed loss of 20 dB. A data matrix Z gives their exact locations with respect to the position of the transmitter (0, 0).

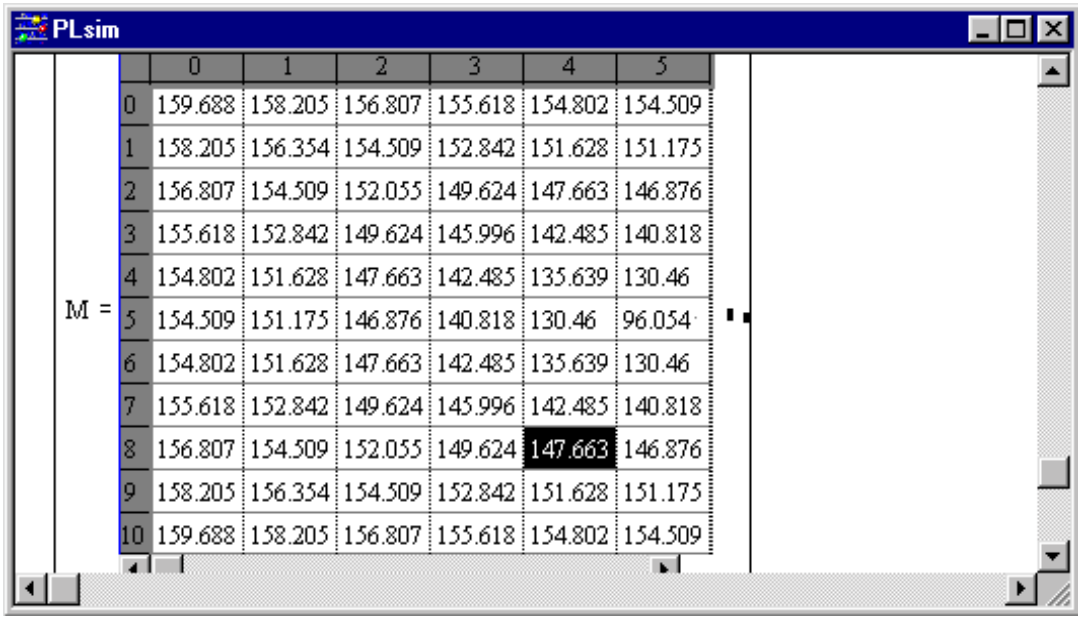

	0	1	2	3	4	5
0	159.688	158.205	156.807	155.618	154.802	154.509
1	158.205	156.354	154.509	152.842	151.628	151.175
2	156.807	154.509	152.055	149.624	147.663	146.876
3	155.618	152.842	149.624	145.996	142.485	140.818
4	154.802	151.628	147.663	142.485	135.639	130.46
5	154.509	151.175	146.876	140.818	130.46	96.054
6	154.802	151.628	147.663	142.485	135.639	130.46
7	155.618	152.842	149.624	145.996	142.485	140.818
8	156.807	154.509	152.055	149.624	147.663	146.876
9	158.205	156.354	154.509	152.842	151.628	151.175
10	159.688	158.205	156.807	155.618	154.802	154.509

Figure 4.4 Truncated 11×11 matrix M.

The addition of M and Z gives the total path loss matrix T. However, in order to display this result as a contour plot in its correct perspective, the following steps must be taken to combat an apparent Mathcad default feature:

- flip T matrix about x-axis
- transpose said result

These programming steps are shown in Figure 4.5.

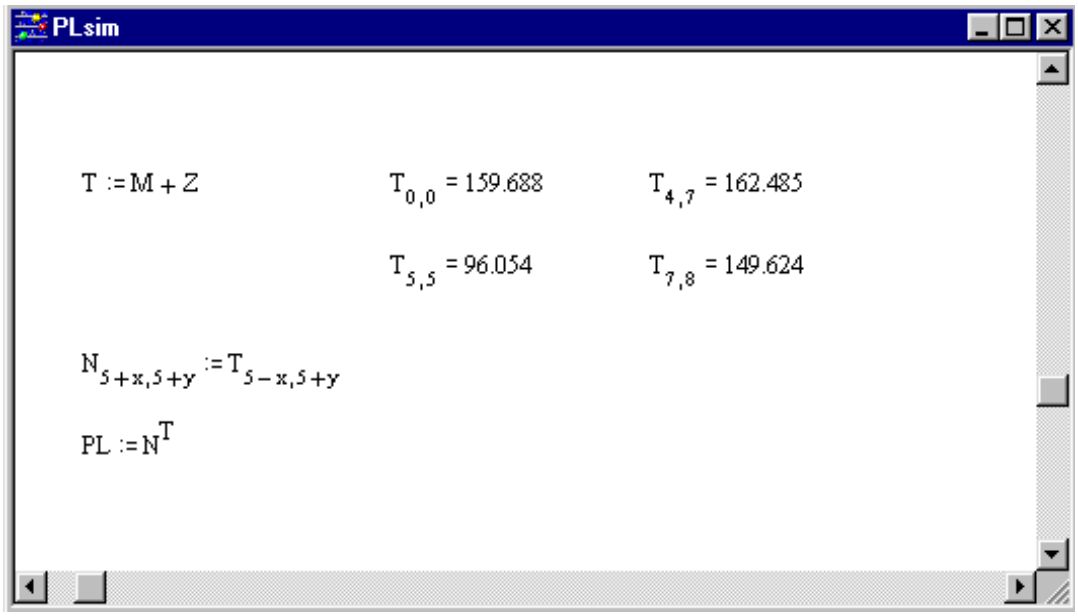

Figure 4.5 Programming steps to facilitate Mathcad default feature.

The data matrix Z, as shown in Figure 4.6, actually represents simulated terrain data. However, in the real world of signal propagation this matrix will be much more

detailed in terms of obstruction losses over an entire area. A typical urban environment will also require a grid resolution far greater than 1 km to simulate obstruction positions with some degree of accuracy.

PLsim

$Z =$

	0	1	2	3	4	5	6	7	8	9	10
0	0	0	0	0	0	0	0	0	0	0	0
1	0	0	0	0	0	0	0	0	0	0	0
2	0	20	20	0	0	0	20	20	20	0	0
3	0	0	0	20	0	0	20	20	20	0	0
4	0	0	0	0	20	0	20	20	20	0	0
5	20	0	0	0	0	0	0	0	0	0	0
6	0	20	20	0	0	0	0	0	0	0	0
7	0	20	20	0	0	0	0	0	0	0	0
8	0	0	0	0	0	20	0	20	20	0	0
9	0	0	20	0	0	0	0	20	20	20	0
10	0	0	0	0	0	0	0	20	20	20	0

Figure 4.6 Data matrix Z .

Figure 4.7 shows the simulated PL contour plot for the Hata-Okumura model with added obstructions. Using the auto contour feature, Mathcad software displays actual path loss over the 10×10 km square simulated propagation area. The apparent elastic nature of the contour lines gives a good reproduction of signal propagation around obstructions. The numbered contour lines give an indication of the path loss value in a particular region relative to the center of the grid.

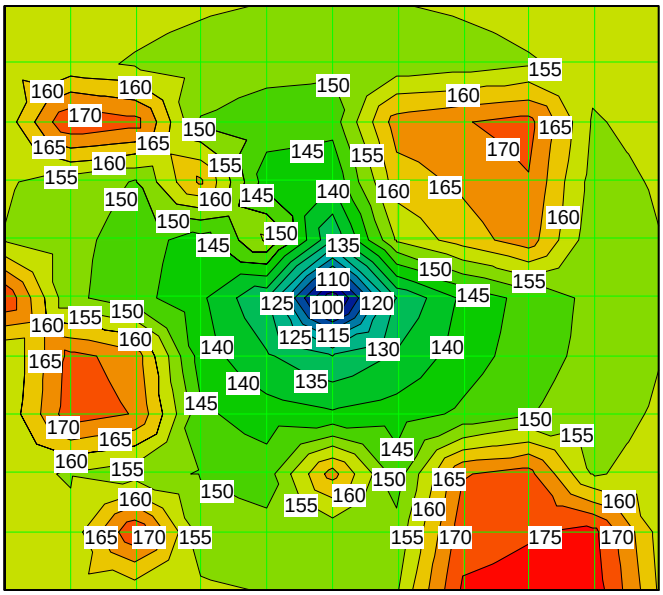

PL

Figure 4.7 Simulated PL contour plot for the Hata-Okumura model with added obstructions.

4.1.2 BER Simulation

Using link analysis a DS spread spectrum system using BPSK modulation is simulated. A link is defined as the channel or region between the transmitter and receiver. The primary purpose of a link analysis is to determine the actual system operating point and to establish that the bit error probability or bit error rate (BER) associated with that point is less than or equal to the system requirement [Sklar, 1988].

In evaluating system performance, the quantity of greatest interest is the signal-to-noise ratio, SNR. This is because the basic system design centers on the ability to detect a signal with acceptable BER. Since a BPSK modulated signal is used in this simulation,

the signal-to-noise ratio can be expressed as a carrier power-to-noise ratio P_rNR. An equation for P_rNR is obtained by dividing the Friis free space equation, given as Equation (2.1), by noise power N, and as such

$$\frac{P_r}{N} = \frac{EIRP\, G_r/N}{L_S\, L} \tag{4.2}$$

where $EIRP$ is the transmitted signal power, and L_S is the path loss or space loss. For digital communication links it is common to replace noise power N with noise power spectral density N_o, given as

$$N_o = kT \tag{4.3}$$

where k is Boltzmann's constant (1.38×10^{-23} joule/K), and T the system effective temperature in degrees kelvin, which is a function of the noise radiated into the antenna and the thermal noise generated within the first stages of the receiver. Equation (4.2) then becomes

$$\frac{P_r}{N_o} = \frac{EIRP\, G_r/T}{k\, L_S\, L} \tag{4.4}$$

where G_r/T is called the receiver figure of merit. Assuming that all the received power will be in the BPSK modulating signal we can say

$$\frac{P_r}{N_o} = \frac{S}{N_o} = \frac{E_b}{N_o} \cdot R_b \tag{4.5}$$

where S is the average modulating signal power, E_b/N_o the bit energy per noise power spectral density, and R_b the bit rate. As implied earlier, in link analysis a safety margin or link margin M is first established, here it is introduced as

$$\frac{P_r}{N_o} = \left(\frac{E_b}{N_o}\right)_{rec} \cdot R_b = M \cdot \left(\frac{E_b}{N_o}\right)_{reqd} \cdot R_b \tag{4.6}$$

where $(E_b/N_o)_{rec}$ is received E_b/N_o, and $(E_b/N_o)_{reqd}$ is required E_b/N_o. The difference in decibels between $(E_b/N_o)_{rec}$ and $(E_b/N_o)_{reqd}$ gives the actual link margin:

$$M = \left(\frac{E_b}{N_o}\right)_{rec} - \left(\frac{E_b}{N_o}\right)_{reqd} \tag{4.7}$$

Combining Equations (4.4) and (4.6) and solving for the link margin M, yields

$$M = \frac{EIRP\, G_r/T}{(E_b/N_o)_{reqd}\, R_b\, k\, L_s\, L} \tag{4.8}$$

This equation expressed now in decibels is given as

$$M = EIRP + G_r - (E_b/N_o)_{reqd} - R_b - kT - L_s - L \tag{4.9}$$

where $EIRP$ is in decibel-watts (dBW); N_o is in decibel-watts per hertz (dBW/Hz); G_r is in decibels referenced to isotropic gain (dBi); R_b is in decibels referenced to 1 bit/s (dB-bit/s) and all other terms in decibels (dB). In the BER simulation however, Equation (4.9) is expressed as Equation (4.10) since $(E_b/N_o)_{rec}$ is a function of path loss L_s.

$$\left(\frac{E_b}{N_o}\right)_{rec} = EIRP + G_r - R_b - kT - L_s - L \tag{4.10}$$

The bit error probability for BPSK signaling is given by Sklar [13] as

$$P_b = Q\left(\sqrt{\frac{2E_b}{N_o}}\right) \tag{4.11}$$

where the Q function is defined as

$$Q(x) = 0.5\left(1 - erf\left(\frac{x}{\sqrt{2}}\right)\right) \tag{4.12}$$

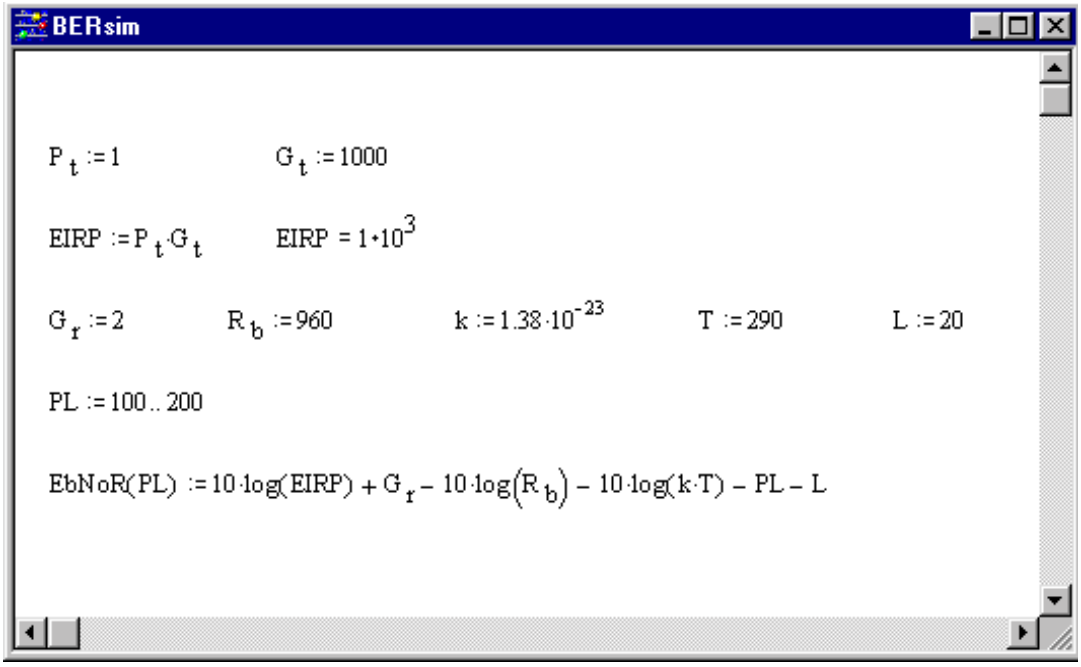

Figure 4.8 Parameters used in plotting BER curve.

The parameters used in plotting a BER curve are shown in Figure 4.8, where P_t is the transmitting power given as 1 W, and G_t the transmitting antenna gain. Note here that $(E_b/N_o)_{rec}$, expressed as $EbNoR$ in the Mathcad program is defined as a function of PL over a range of 100 to 200 dB. The Q function $Q(x)$ is given as $Q(EbNoR(PL))$, where a value of 0 is returned for $Q(EbNoR(100))$ and a value of 1 for $Q(EbNoR(200))$ within the specified range of path loss values. This gives a good indication as to how SNR limits are set in actual system design, since BER curves describe a system in terms of available E_b/N_o. The actual plot is shown in Figure 4.9.

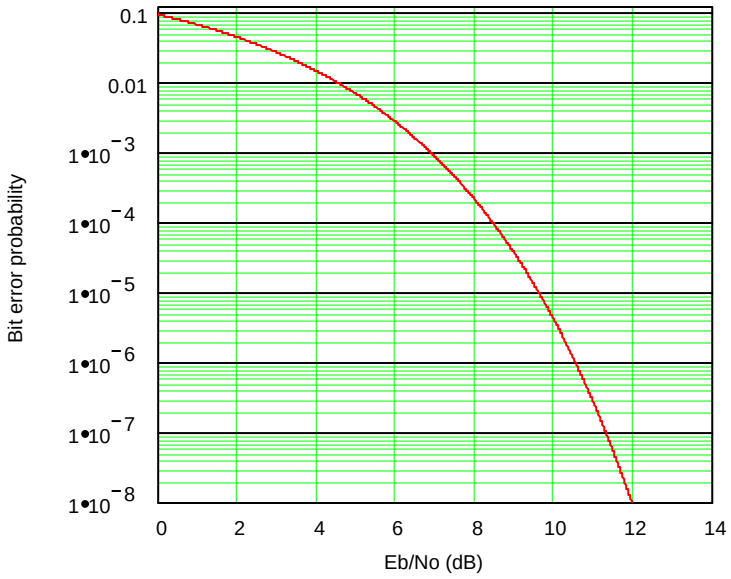

Figure 4.9 BER plot for simulated data shown in Figure 4.8.

Based on parameters shown in Figure 4.10 a contour plot was generated using the Hata-Okumura model with obstruction. The data matrix M used in plotting this graph was executed from a relatively long Mathcad program of If statements. This matrix, which gives a good indication of bit error probability over the simulated terrain, is shown in Figure 4.11. From the data one can interpret that for an acceptable bit error probability, say between 10^{-5} and 10^{-8}, the radial distance for a receiver from the transmitter position must be less than 2 kilometers. However, a keen observation in this particular simulation is the dramatic effect of varying values of G_r, R_b and L. This concept plays well in designing a communication link.

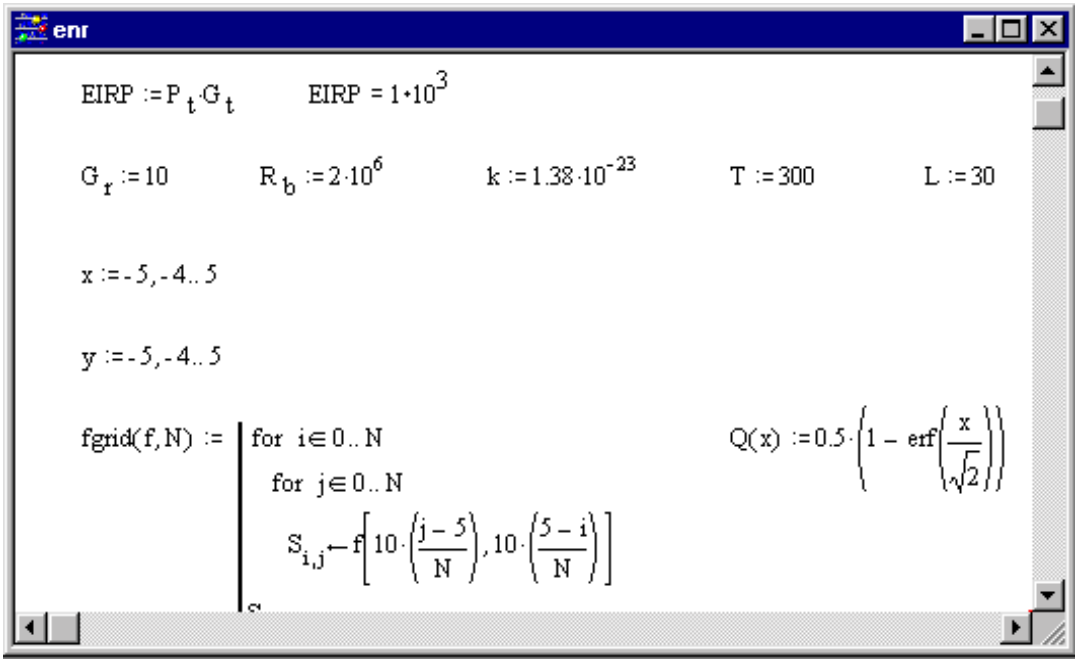

Figure 4.10 Parameters used in generating BER contour plot.

The general idea of BER contour plotting is a relatively new one, most simulations of signal propagation coverage use field strength or path loss as their displayed parameter. The Mathcad generated BER contour plot shown in Figure 4.12, is a good picture representation of the simulated terrain data. Note that the picture is shown here with color shading.

Bit error probability or bit error rate (BER) may be fully understood by considering the case of a digital communication system that has at its output, a sequence of symbols. The output of the system due to the influence of channel noise (which is assumed Gaussian) will be a different sequence of bits. In an ideal or noiseless system,

both input and output sequences are the same, but in a practical system, they will occasionally differ. Therefore, the bit error probability may be defined as the probability that the input sequence of symbols is not equal to the output sequence of symbols. In a practical digital communication system, the values of bit error probability range from 10^{-4} to 10^{-7}. In practice, the bit error rate (BER) is used together with time intervals to provide performance objectives for digital systems, as stated in Townsend [6]. One example of a performance objective statement is as follows:

- A BER of less than 1: 10^{-6} for a time interval of 1 minute.

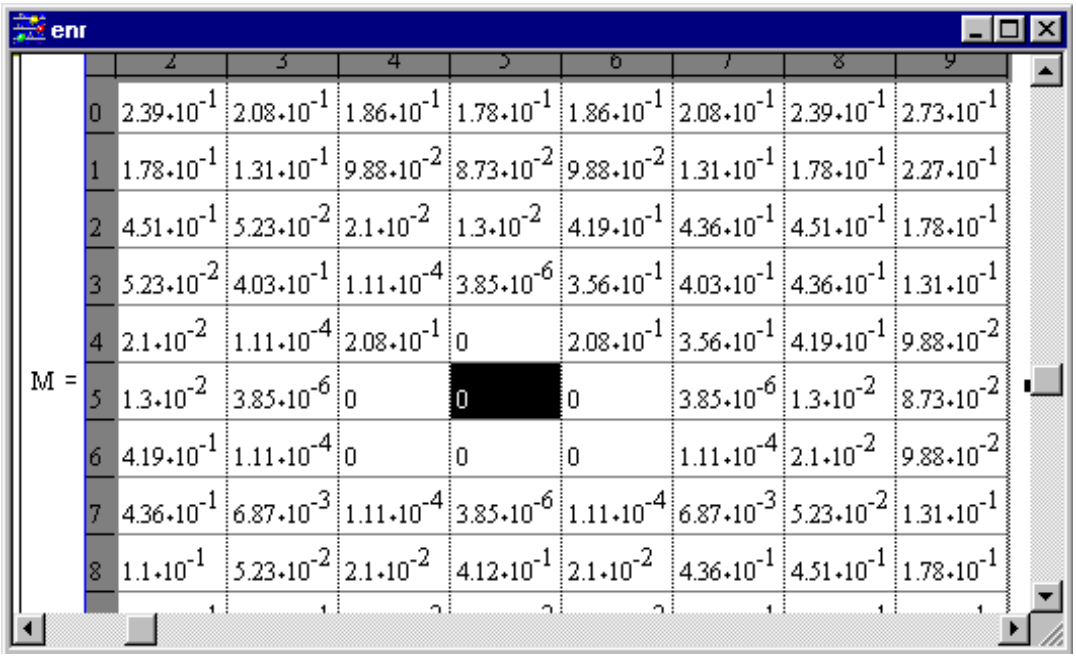

	2	3	4	5	6	7	8	9
0	$2.39\cdot10^{-1}$	$2.08\cdot10^{-1}$	$1.86\cdot10^{-1}$	$1.78\cdot10^{-1}$	$1.86\cdot10^{-1}$	$2.08\cdot10^{-1}$	$2.39\cdot10^{-1}$	$2.73\cdot10^{-1}$
1	$1.78\cdot10^{-1}$	$1.31\cdot10^{-1}$	$9.88\cdot10^{-2}$	$8.73\cdot10^{-2}$	$9.88\cdot10^{-2}$	$1.31\cdot10^{-1}$	$1.78\cdot10^{-1}$	$2.27\cdot10^{-1}$
2	$4.51\cdot10^{-1}$	$5.23\cdot10^{-2}$	$2.1\cdot10^{-2}$	$1.3\cdot10^{-2}$	$4.19\cdot10^{-1}$	$4.36\cdot10^{-1}$	$4.51\cdot10^{-1}$	$1.78\cdot10^{-1}$
3	$5.23\cdot10^{-2}$	$4.03\cdot10^{-1}$	$1.11\cdot10^{-4}$	$3.85\cdot10^{-6}$	$3.56\cdot10^{-1}$	$4.03\cdot10^{-1}$	$4.36\cdot10^{-1}$	$1.31\cdot10^{-1}$
4	$2.1\cdot10^{-2}$	$1.11\cdot10^{-4}$	$2.08\cdot10^{-1}$	0	$2.08\cdot10^{-1}$	$3.56\cdot10^{-1}$	$4.19\cdot10^{-1}$	$9.88\cdot10^{-2}$
5	$1.3\cdot10^{-2}$	$3.85\cdot10^{-6}$	0	0	0	$3.85\cdot10^{-6}$	$1.3\cdot10^{-2}$	$8.73\cdot10^{-2}$
6	$4.19\cdot10^{-1}$	$1.11\cdot10^{-4}$	0	0	0	$1.11\cdot10^{-4}$	$2.1\cdot10^{-2}$	$9.88\cdot10^{-2}$
7	$4.36\cdot10^{-1}$	$6.87\cdot10^{-3}$	$1.11\cdot10^{-4}$	$3.85\cdot10^{-6}$	$1.11\cdot10^{-4}$	$6.87\cdot10^{-3}$	$5.23\cdot10^{-2}$	$1.31\cdot10^{-1}$
8	$1.1\cdot10^{-1}$	$5.23\cdot10^{-2}$	$2.1\cdot10^{-2}$	$4.12\cdot10^{-1}$	$2.1\cdot10^{-2}$	$4.36\cdot10^{-1}$	$4.51\cdot10^{-1}$	$1.78\cdot10^{-1}$

Figure 4.11 Data matrix M, used in generating BER contour plot.

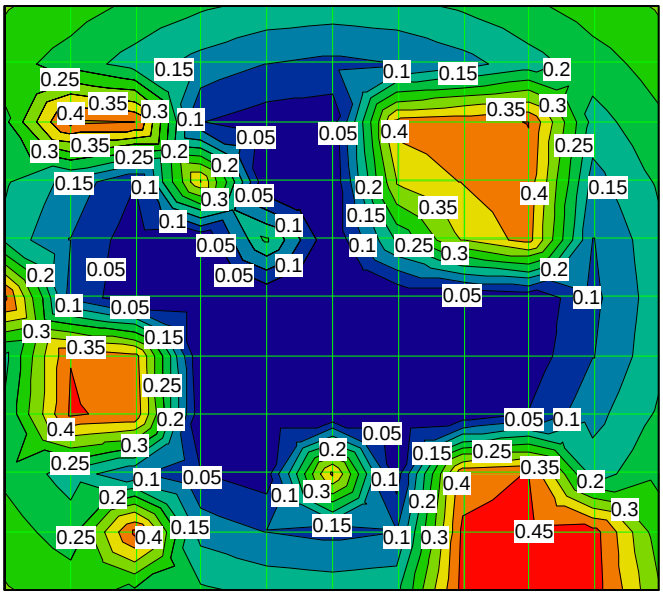

Figure 4.12 Mathcad generated BER contour plot based on the Hata-Okumura model with added obstructions.

In a CDMA multi-user environment, with k users, it can be shown that the bit error probability increases drastically after a certain value of k. Therefore, in designing a digital communication system this factor also has to be taken into consideration.

4.2 Miami Propagation Measurements

In developing a RF propagation model for a DS spread spectrum communication system, radio propagation measurements (at 2.4 GHz) were taken in Dade county, Miami. A particular area called the Ives Estates was targeted for adequate propagation

measurements. This urban area was somewhat close to the Golden Glades interchange. However, since this model at this point is based on line-of-sight measurements, linear propagation measurements were also taken along Alligator alley, a straight stretch of highway I-75. These linear propagation measurements of signal strength in decibel-milliwatts (dBm) vs. distance in meters (m) were integrated into a Mathcad program in order to generate a scatter plot used in its regression analysis. The estimated Mathcad fitted curve was then used in establishing a standard formula for the RF propagation model, based on derivations used in the Hata-Okumura model [2].

4.2.1 Hata-Okumura Model Based Derivations

According to Hata [2], the propagation loss in an urban area can be presented as a simple form, given by

$$A + B \log_{10} d \tag{4.13}$$

where A and B are frequency and antenna height dependent functions, and d is the distance. Note here, Hata has also reiterated the established theory that propagation loss shows logarithmic behavior to the distance. Based on this simple form, Hata developed an empirical formula based on the free space propagation model.

In free space, the received power density is given as Equation (4.14) where η is the intrinsic impedance of free space taken as 120 π ohms. This equation can therefore be rewritten as Equation (4.15).

$$P_d = \frac{EIRP}{4\pi d^2} = \frac{E^2}{\eta} \tag{4.14}$$

$$P_d = \frac{|E|^2}{120\pi} \tag{4.15}$$

where $|E|$ represents the magnitude of the radiating portion of the electric field in the far field, E is in V/m and P_d in W/m^2. Converting Equation (4.15) into dBs, we have

$$10\log_{10} P_d = 20\log_{10} E - 10\log_{10}(120\pi) \tag{4.16}$$

or simply

$$P_d = E - 10\log_{10}(120\pi) \tag{4.17}$$

where P_d is now in dBW/m^2 and E in dBV/m; converting these units into practical units of dBm/m^2 and dBμV/m respectively gives

$$P_d = E - 10\log_{10}(120\pi) - 90 \tag{4.18}$$

since dBm/m^2 = dBW/m^2 + 30 and dBμV/m = dBV/m + 120

Received power is given as

$$P_r = P_d \cdot A_e \tag{4.19}$$

where A_e is the absorption cross section of an isotropic antenna, given as

$$A_e = \frac{\lambda^2}{4\pi} \tag{4.20}$$

Equation (4.19) can now be expressed as

$$P_r = E + 10\log_{10}\left(\lambda^2/4\pi\right) - 115.76 \tag{4.21}$$

where P_r is in dBm. Propagation loss is the difference value between the radiated power and the received power, using Equation (4.21) gives

$$\begin{aligned} PL &= P_t - P_r \\ &= P_t - E - 10\log_{10}\left(\lambda^2/4\pi\right) + 115.76 + 30 \end{aligned}$$

$$PL = P_t - E - 10\log_{10}\left(\lambda^2/4\pi\right) + 145.76 \tag{4.22}$$

where P_t is in dBW and PL in dB.

The HP8648C Signal Generator used as a transmitter indicated a maximum output level of 14.5 dBm (referenced) for a 2.4 GHz transmitted signal. Converting this output into milliwatts gives a transmitted power level of approximately 30 mW. Therefore the 30 mW: ERP/dipole needs to be transformed to EIRP. This transformation is accomplished by adding the difference value for power gain between the isotropic antenna and the dipole antenna taken as 2.2 dB. As such P_t can be equated as

$$P_t = P_{t'} + 2.2 \tag{4.23}$$

where $P_{t'}$ is 30 mW: ERP/dipole, this gives P_t (dBW: EIRP) as –13.03 dB. Substituting for P_t in Equation (4.22) gives

$$PL = 132.73 - E - 10\log_{10}\left(\lambda^2/4\pi\right) \tag{4.24}$$

Hata [2] at this point introduced Okumura's median field strength curves into the derivations. Generated curves of field strength vs. distance for various mobile antenna and base station heights are used in deriving values for the constants shown in Equation (4.25). Where α and β are the constants determined by h_b (m) and f (MHz). This equation is based on the logarithmic shape of the field strength curves, and is given as

$$E = \alpha + \beta \log_{10} d \tag{4.25}$$

Therefore, once values for these constants are established; Equation (4.25) can be substituted into Equation (4.24) resulting in the final PL empirical formula, Equation (4.26). Based on the data collected from the Miami propagation measurements, α and β will have to be derived from the linear propagation measurements taken (a single median field strength curve) at a transmission frequency of 2.4 GHz with relatively fixed mobile and transmitter antenna heights of 5 meters. The HP8596E Spectrum Analyzer used as a receiver here displayed received signal levels in dBm, in order to facilitate the use of Equation (4.25) this measured data will be converted to dBμV/m.

$$PL = 161.78 - \alpha - \beta \log_{10} d \tag{4.26}$$

4.2.2 Linear Measured Data

With the HP8648C Signal Generator located at the differential global positioning system (DGPS) radio reading of longitude W80^{o}35’27.4” and latitude N26^{o}08’45.9”, linear propagation measurements were taken along Alligator alley. These measurements taken approximately every 50 meters covered a total approximate distance of 1800 meters. The mobile unit’s position readings were recorded with both DGPS and GPS radios for comparison purposes. Table 4.1 gives the mobile unit’s position readings vs. the received signal strength as displayed on the HP8596E Spectrum Analyzer.

In order to express the tabulated data in the form of field strength E vs. distance d, signal strength readings in dBm were converted to dBμV/m using Equation (4.21) and

the mobile unit's DGPS reading relative to the transmitter location into distance in meters using a devised Mathcad conversion program.

Table 4.1 Propagation measurements taken along Alligator alley.

DGPS	GPS	Signal Strength
N26°08'46.1" W 80°35'25.9"	N26°08'46.0" W 80°35'25.6"	-30dBm
N26°08'46.0" W 80°35'23.2"	N26°08'46.1" W 80°35'23.2"	-40dBm
N26°08'46.0" W 80°35'16.8"	N26°08'46.0" W 80°35'16.5"	-55dBm
N26°08'46.0" W 80°35'13.4"	N26°08'46.2" W 80°35'12.6"	-58dBm
N26°08'46.0" W 80°35'10.0"	N26°08'46.4" W 80°35'09.1"	-62dBm
N26°08'46.0" W 80°35'00.8"	N 25°57'46.8" W 80°09'00.6"	-65dBm
N 26°08'46.0" W 80°34'58.4"	N 26°08'46.5" W 80°34'59.5"	-75dBm
N 26°08'45.9" W 80°34'54.6"	N 26°08'46.0" W 80°34'55.7"	-66dBm
N 26°08'45.9" W 80°34'50.8"	N 26°08'46.1" W 80°34'51.3"	-70dBm
N 26°08'46.0" W 80°34'47.1"	N 26°08'46.1" W 80°34'47.0"	-77dBm
N 26°08'46.0" W 80°34'44.0"	N 26°08'46.2" W 80°34'43.7"	-80dBm
N 26°08'46.0" W 80°34'36.4"	N 26°08'46.2" W 80°34'36.6"	-75dBm
N 26°08'45.9" W 80°34'34.5"	N 26°08'46.5" W 80°34'34.5"	-80dBm
N 26°08'45.9" W 80°34'30.2"	N 26°08'46.6" W 80°34'30.8"	-79dBm

- Table recorded on 7-17-1998.

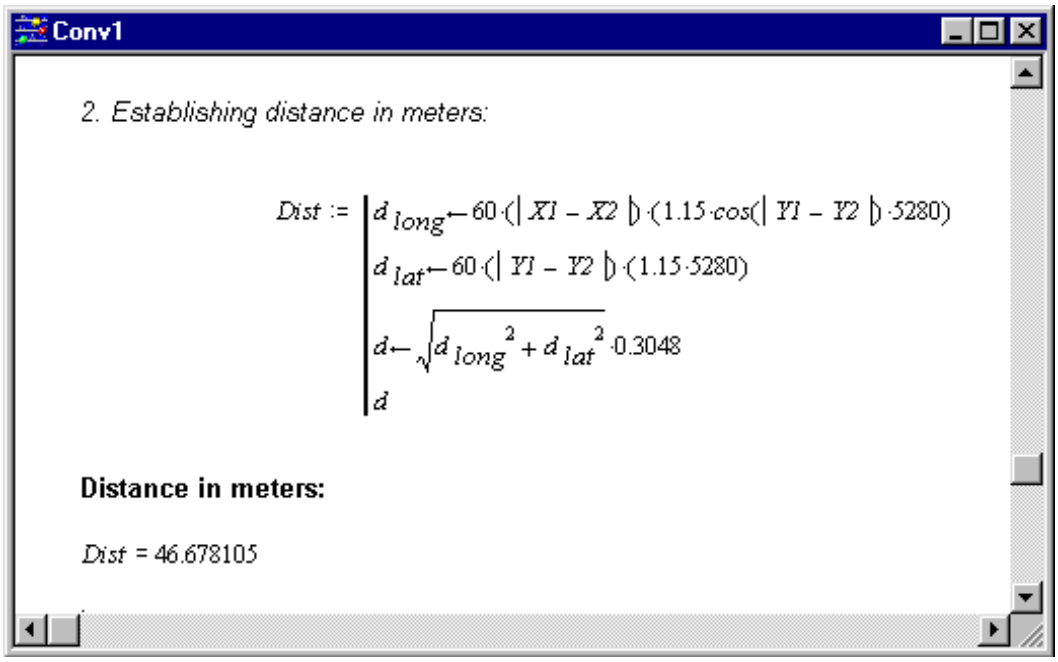

Figure 4.13 Part of Mathcad program used in calculating distances between longitudes and latitudes.

4.2.2.1 Distance Calculation

An encyclopedia definition gives latitude and longitude as a system of geometrical coordinates used in designating the location of places on the Earth's surface. Latitude gives the location of a place north or south of the equator by angular measurements ranging from 0^o at the equator to 90^o at the poles. Longitude gives the location of a place east or west of the north-south line called the prime meridian by angular measurements ranging from 0^o at the prime meridian to 180^o at the International Date Line.

In most mapping software including MapInfo, positions of longitude and latitude are often referred to as X and Y positions. Therefore, since circles of longitude and latitude are actually orthogonal, they can be regarded as comprising a XY plane. Based on this theory relatively short distances between two locations of longitude and latitude can be calculated using the Pythagoras theorem, that is $d^2 = x^2 + y^2$. This concept holds well with MapInfo as a 0.053% difference was observed in distance calculations. Chew [15] gives the distances between latitudes as 1.15 miles for every 1 minute, and distances between longitudes as 1.15 cosine (latitude) miles for every 1 minute.

The first stage of the devised Mathcad conversion program, shown in Figure 4.13, converts degree/minute/second coordinates into decimal degrees. Point locations are then referred to as X1, Y1 and X2, Y2. The second stage of the conversion program returns the distance in meters.

4.2.2.2 Regression Analysis

The measured data set of field strength vs. distance is shown in Figure 4.14. This data set is used to generate a scatter plot as shown in Figure 4.15. A scatter plot basically gives an insight of the propagation channel in terms of its critical spots. An analysis of this scatter plot reveals that after approximately 800 meters, the transmitted signal begins to experience the effects of multipath. This is reflected in the random variation of field strength between distances of 800 and1800 meters. On an overall basis, the scatter plot does indicate logarithmic behavior to the distance and as such, a regression model can be established based on Equation (4.25).

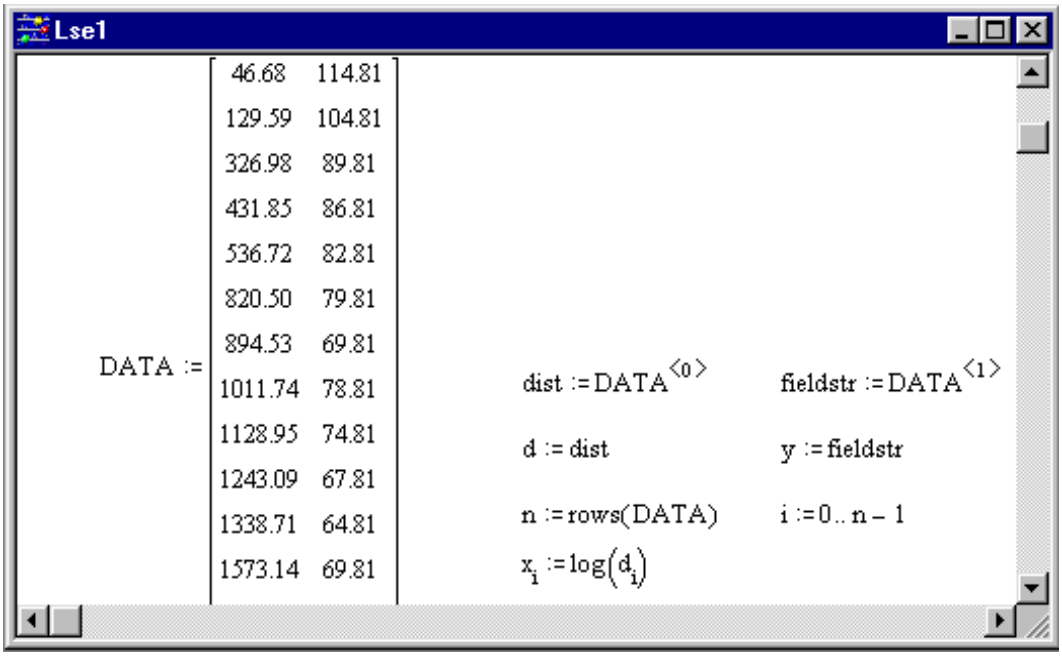

Figure 4.14 Measured data set of field strength vs. distance.

A simple regression model is given as the Equation (4.27) where α and β are now the best estimators of the curve that best fits the data points. One way of minimizing the distance between the proposed regression curve and the data points is by the method of least squares. In this method the distance to be minimized called the residual error e_i is given as Equation (4.28).

$$y_i = \alpha + \beta \cdot x_i \tag{4.27}$$

$$e_i = y_i - (\alpha + \beta \cdot x_i) \tag{4.28}$$

One solution of the regression analysis is the sum of the squared residuals given as Equation (4.29). To find the values of α and β that minimize the sum of the squares a little calculus is used. If the sum of the squares has a minimum, it will occur where the partial derivatives with respect to α and β equal zero. Using the fact that the derivative of a sum is the sum of the derivatives, we can find a system of equations and ultimately the least square estimates.

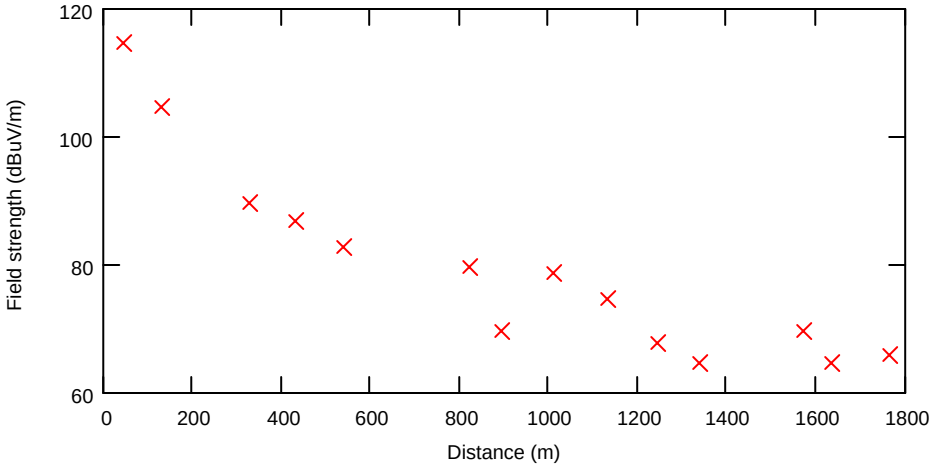

Figure 4.15 Mathcad generated scatter plot.

$$SSE(\alpha,\beta)=\sum_{i}\left[y_i-(\alpha+\beta\cdot x_i)\right]^2 \tag{4.29}$$

Taking the partial derivative of Equation (4.29) with respect to α gives Equation (4.30) and setting the results equal to zero gives Equation (4.31).

$$\sum_i \left[\frac{d}{d\alpha} \left[y_i - (\alpha + \beta \cdot x_i) \right]^2 \right]$$

yields $$\sum_i \left(-2 \cdot y_i + 2 \cdot \alpha + 2 \cdot \beta \cdot x_i \right) \tag{4.30}$$

$$-2 \cdot \left(\sum_i y_i \right) + 2 \cdot \beta \cdot \left(\sum_i x_i \right) + 2 \cdot n \cdot \alpha = 0$$

yields $$n \cdot \alpha + \beta \cdot \left(\sum_i x_i \right) = \sum_i y_i \tag{4.31}$$

Taking the partial derivative of Equation (4.29) with respect to β gives Equation (4.32) and setting the results equal to zero gives Equation (4.33).

$$\sum_i \left[\frac{d}{d\beta} \left[y_i - (\alpha + \beta \cdot x_i) \right]^2 \right]$$

yields $$\sum_i \left(-2 \cdot \left(y_i - \alpha - \beta \cdot x_i \right) \cdot x_i \right) \tag{4.32}$$

$$-2\cdot\left(\sum_i\left(x_i\cdot y_i\right)\right)+2\cdot\beta\left(\sum_i\left(x_i\right)^2\right)+2\cdot\alpha\left(\sum_i x_i\right)=0$$

yields

$$\alpha\cdot\left(\sum_i x_i\right)+\beta\cdot\left(\sum_i\left(x_i\right)^2\right)=\sum_i\left(x_i\cdot y_i\right) \tag{4.33}$$

Equation (4.31) and Equation (4.33) are called the normal equations for the regression. A solution to these equations can be obtained using Mathcad. Therefore, for $y_i = E_i$ and $x_i = log\, d_i$, the solution is given as shown in Figure 4.16.

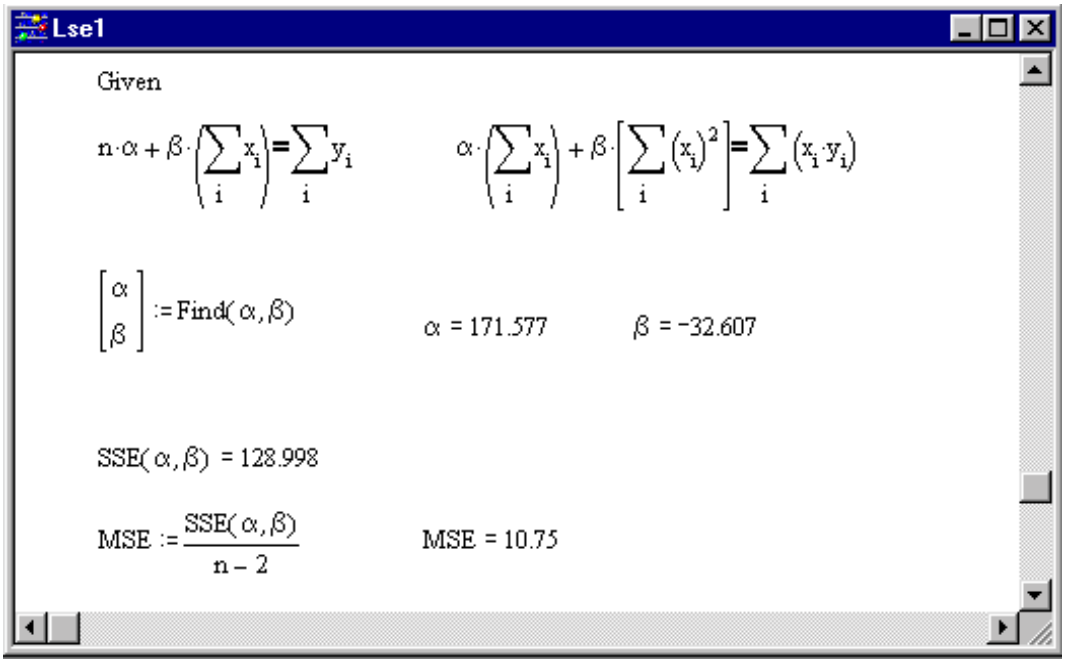

Figure 4.16 Regression analysis solution.

The returned values for α and β are the least square estimates for the smallest possible sum of squares given as $SSE(\alpha,\beta)$. The smaller the value of $SSE(\alpha,\beta)$, the closer the regression curve fits the data points. The mean square error MSE gives the population error variance. An estimate of MSE for the sample size n is calculated by dividing the value of SSE by $(n-2)$, since they are two parameters being estimated. Figure 4.17 shows the graphical results of the regression analysis.

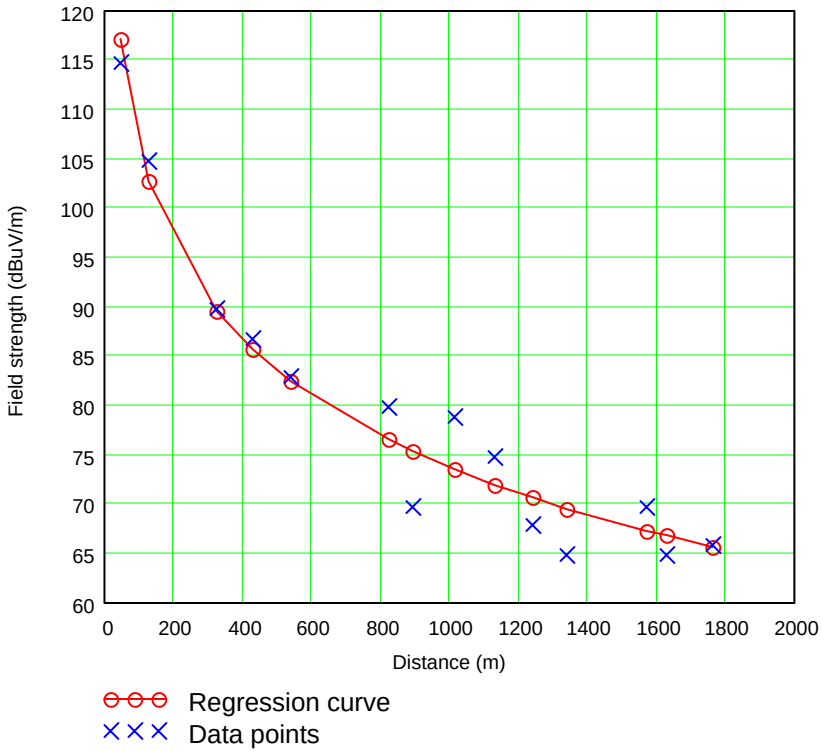

.

Figure 4.17 Graphical results of the regression analysis.

A plot of path loss vs. distance for the proposed 2.4 GHz propagation model is shown in Figure 4.18. This is based on a transmitter power of 30 mW: ERP/dipole and antenna gains of 12 dB.

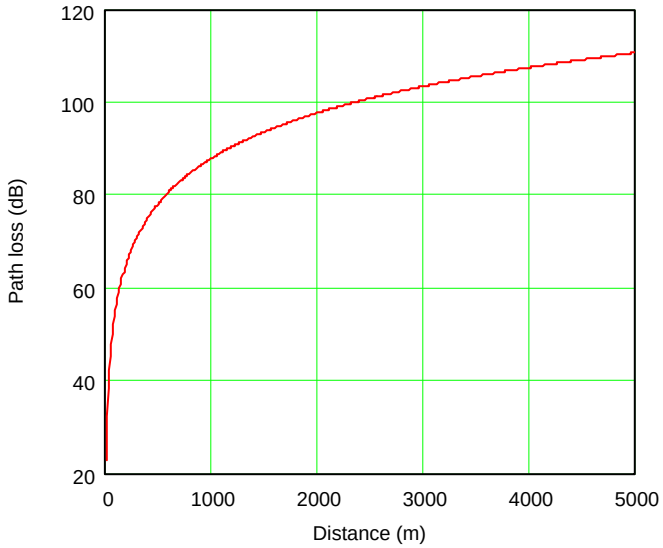

Figure 4.18 Path loss predictions at 2.4 GHz.

4.2.3 Random Measured Data

A set of random, line-of-sight (LOS) propagation measurements were taken in the Ives Dairy Estates area. These measurements taken along Ives Dairy road covered a relatively small urban area. The transmitter positioned at longitude W80^{o}10’0.3” and latitude N25^{o}57’54.5”, was located on the roof of a nearby 10 meter building. In order to facilitate adequate LOS communications, the mobile unit was mounted on a bucketed

truck. By using a cellular telephone to relay panning information, pointing losses between the directional antennas were minimized. Propagation measurements of signal strength vs. distance were then tabulated as shown in Table 4.2.

Table 4.2 Propagation measurements taken along Ives Dairy road.

DGPS	GPS	Signal Strength
N25°57’46.7” W80°09’47.3”	N25°57’46.6” W80°09’47.4”	-72dBm
N25°57’46.8” W80°09’41.9”	N25°57’46.9” W80°09’42.4”	-58dBm
N25°57’47.0” W80°09’34.4”	N25°57’47.2” W80°09’34.1”	-67dBm
N25°57’46.3” W80°09’32.3”	N25°57’45.4” W80°09’32.1”	-63dBm
N25°57’46.7” W80°09’30.4”	N25°57’46.1” W80°09’30.5”	-62dBm
N25°57’46.0” W80°09’27.7”	N25°57’45.8” W80°09’28.0”	-70dBm
N25°57’46.7” W80°09’24.7”	N25°57’46.0” W80°09’25.3”	-72dBm
N25°57’46.6” W80°09’21.8”	N25°57’46.9” W80°09’22.2”	-74dBm
N25°57’47.6” W80°09’17.8”	N25°57’45.1” W80°09’17.9”	-80dBm
N25°57’47.1” W80°09’15.3”	N25°57’46.3” W80°09’13.6”	-78dBm
N25°57’46.6” W80°09’21.8”	N25°57’48.5” W80°09’14.7”	-80dBm
N25°57’47.8” W80°09’17.1”	N25°57’47.4” W80°09’18.5”	-81dBm
N25°57’47.4” W80°09’22.4”	N25°57’47.7” W80°09’22.7”	-77dBm

DGPS	GPS	Signal Strength
N25°57’47.4” W80°09’26.6”	N25°57’47.3” W80°09’27.0”	-78dBm
N25°57’47.6” W80°09’29.2”	N25°57’47.0” W80°09’29.8”	-75dBm
N25°57’46.9” W80°09’47.4”	N25°57’47.3” W80°09’47.8”	-58dBm
N25°57’46.7” W80°09’41.9”	N25°57’46.8” W80°09’42.1”	-72dBm
N25°57’46.5” W80°09’24.0”	N25°57’47.0” W80°09’24.9”	-72dBm
N25°57’46.6” W80°09’22.0”	N25°57’46.5” W80°09’22.0”	-75dBm
N25°57’47.5” W80°09’17.1”	N25°57’47.5” W80°09’17.6”	-79dBm
N25°57’47.4” W80°09’21.8”	N25°57’47.5” W80°09’21.2”	-74dBm
N25°57’47.4” W80°09’26.3”	N25°57’47.4” W80°09’26.0”	-74dBm
N25°57’47.7” W80°09’33.2”	N25°57’47.4” W80°09’32.8”	-63dBm
N25°57’47.6” W80°09’38.6”	N25°57’47.7” W80°09’38.5”	-62dBm
N25°57’48.8” W80°09’50.1”	N25°57’48.8” W80°09’50.5”	-55dBm

- Table recorded on 7-15-1998 and 7-16-1998.

For these random propagation measurements a Mathcad program was devised to convert the recorded geographical positions of the mobile unit, referenced to the position of the transmitter, into X and Y distances as shown in Figure 4.19. For example, say a distance between latitudes referenced to the position of the transmitter is 295 meters. Then for a grid resolution of 1/10 km this corresponds to a Y value of 295/100 or 3 to the

nearest grid line. This step is necessary in simulating the propagation coverage plot, since a single position of the mobile unit corresponds to a particular value of signal strength. Using Equation (4.21) these signal strength values in dBm can be converted to field strength values in dBμV/m and subsequently into path loss values by Equation (4.24). Figure 4.20 shows positions of the mobile unit on a 2 × 2 km square map with a grid resolution of 1/10 km. These positions as indicated trace the path taken along Ives Dairy road. Note however with the grid resolution being 1/10 km some positions of the mobile unit overlap.

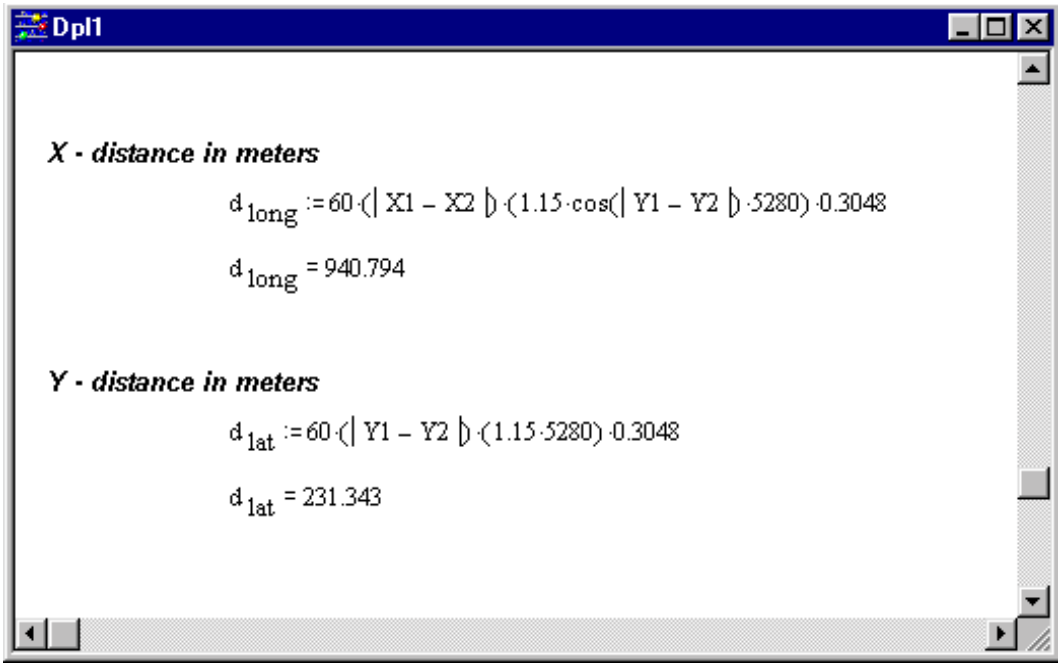

Figure 4.19 Program used in converting geographical positions into X and Y distances.

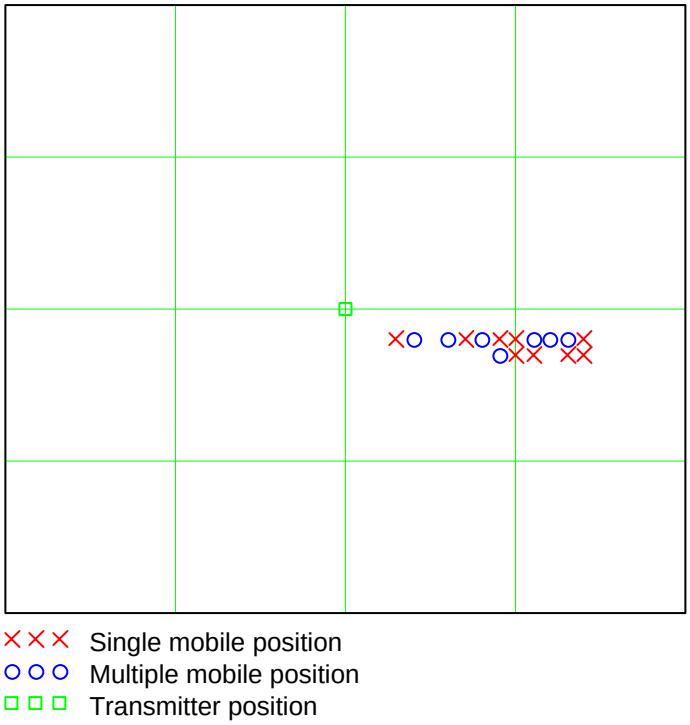

Figure 4.20 Positions of the mobile unit on a 2×2 km square map with a grid resolution of 1/10 km.

4.3 Propagation Coverage Simulation

For a greater degree of accuracy, the propagation coverage for the Ives Dairy Estates area is simulated using a 101×101 PL matrix. A matrix of this order results in a grid resolution of 1/10 km over a 5×5 km square map. Path loss values used in generating this matrix are obtained using the Mathcad program shown in Figure 4.21, which is based on Equation (4.26). This PL matrix as shown in Figure 4.22, gives standard path losses over the terrain as obtained by the Hata-Okumura based derivations.

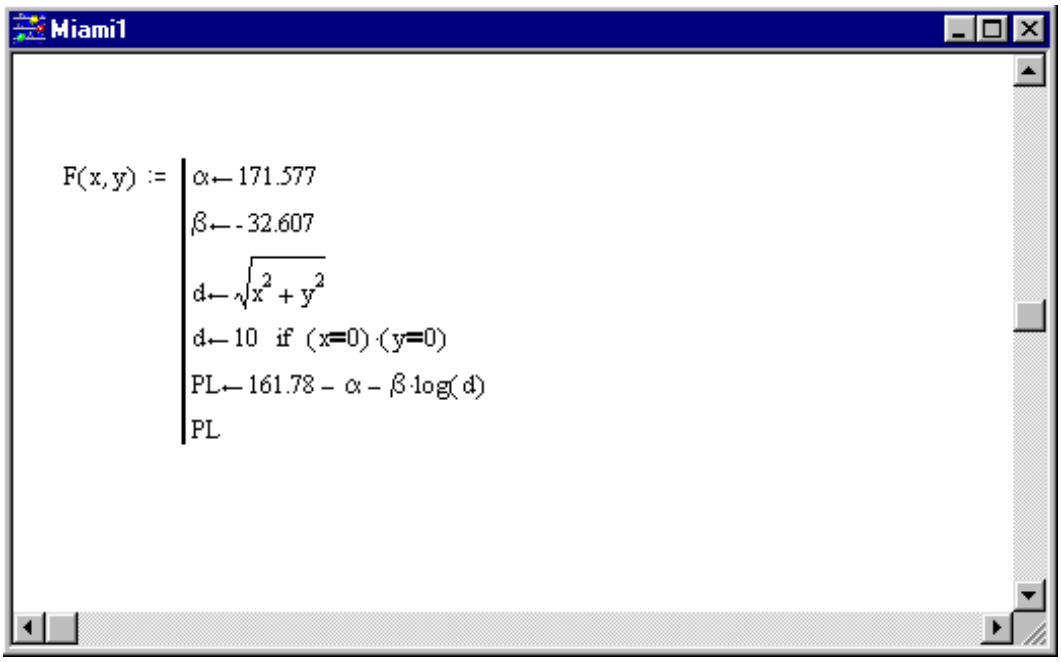

Figure 4.21 Mathcad program used in generating standard path loss values over the terrain.

The regression analysis performed earlier on the linear measured data resulted in a mean square error (MSE) of 10.75, an estimate of the error standard deviation σ, also called the standard error of estimate is given by

$$\sigma = \sqrt{MSE} \tag{4.34}$$

Based on a sample size of 10201, a vector of random numbers is generated from a normal distribution with zero mean μ and standard deviation σ, using a Mathcad built-in

feature. The vector is then packed into an array of size 101×101. This new matrix B is then added to the original PL matrix M, which is defined as

$$M = fgrid(F,100) \tag{4.35}$$

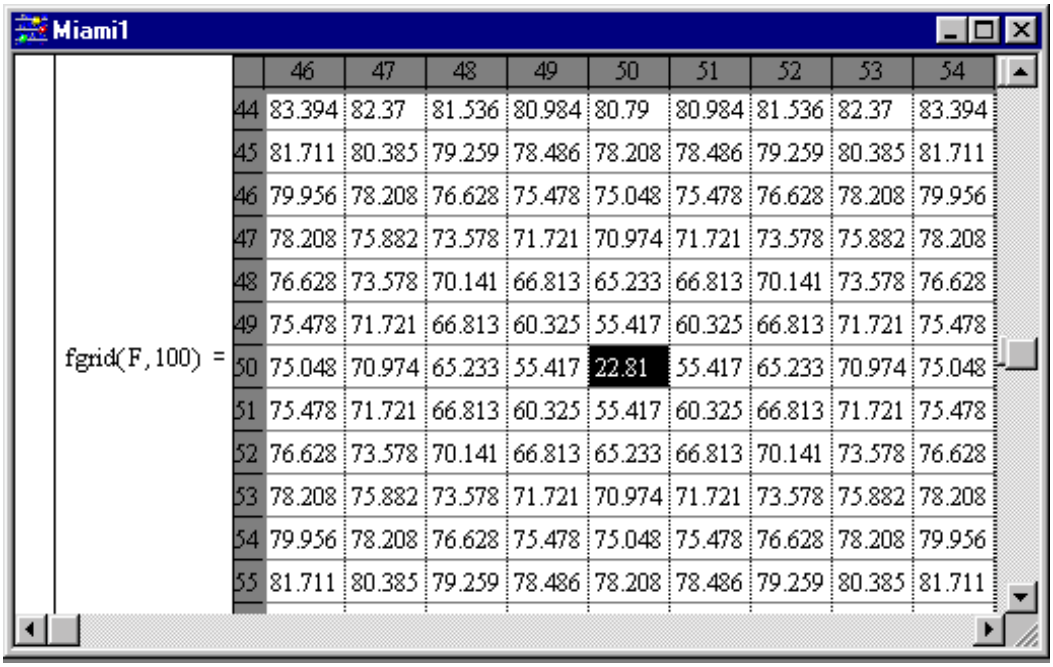

	46	47	48	49	50	51	52	53	54
44	83.394	82.37	81.536	80.984	80.79	80.984	81.536	82.37	83.394
45	81.711	80.385	79.259	78.486	78.208	78.486	79.259	80.385	81.711
46	79.956	78.208	76.628	75.478	75.048	75.478	76.628	78.208	79.956
47	78.208	75.882	73.578	71.721	70.974	71.721	73.578	75.882	78.208
48	76.628	73.578	70.141	66.813	65.233	66.813	70.141	73.578	76.628
49	75.478	71.721	66.813	60.325	55.417	60.325	66.813	71.721	75.478
50	75.048	70.974	65.233	55.417	22.81	55.417	65.233	70.974	75.048
51	75.478	71.721	66.813	60.325	55.417	60.325	66.813	71.721	75.478
52	76.628	73.578	70.141	66.813	65.233	66.813	70.141	73.578	76.628
53	78.208	75.882	73.578	71.721	70.974	71.721	73.578	75.882	78.208
54	79.956	78.208	76.628	75.478	75.048	75.478	76.628	78.208	79.956
55	81.711	80.385	79.259	78.486	78.208	78.486	79.259	80.385	81.711

Figure 4.22 PL matrix giving standard path loss values over the terrain.

The resulting matrix S, defined in Equation (4.36), is then modified to facilitate the set of random propagation measurements taken over the terrain as defined in Figure 4.23.

$$S = M + B \tag{4.36}$$

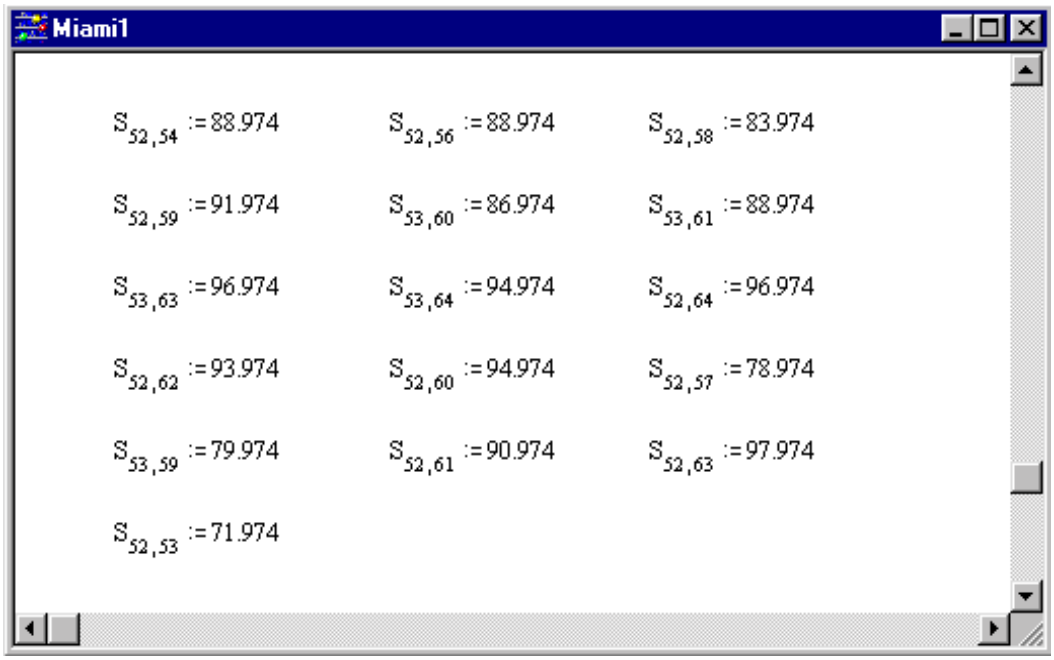

Figure 4.23 Random propagation measurements defined as path loss values.

This matrix S, taken as the final path loss matrix is plotted as shown in Figure 4.24. This simulation of the propagation coverage gives an idea of the path loss in unmeasured areas as well, based on previous analysis. However, in the specific area in question, that is the Ives Dairy road, values of path loss derived based on the random propagation measurements were in the vicinity of those proposed by regression analysis. This indicates that the proposed propagation model is well within acceptable limits. However, recalling that all propagation measurements taken were based on line-of-sight, other propagation measurements are needed based on variable field parameters such as transmitting and receiving antenna heights and speed of the mobile unit.

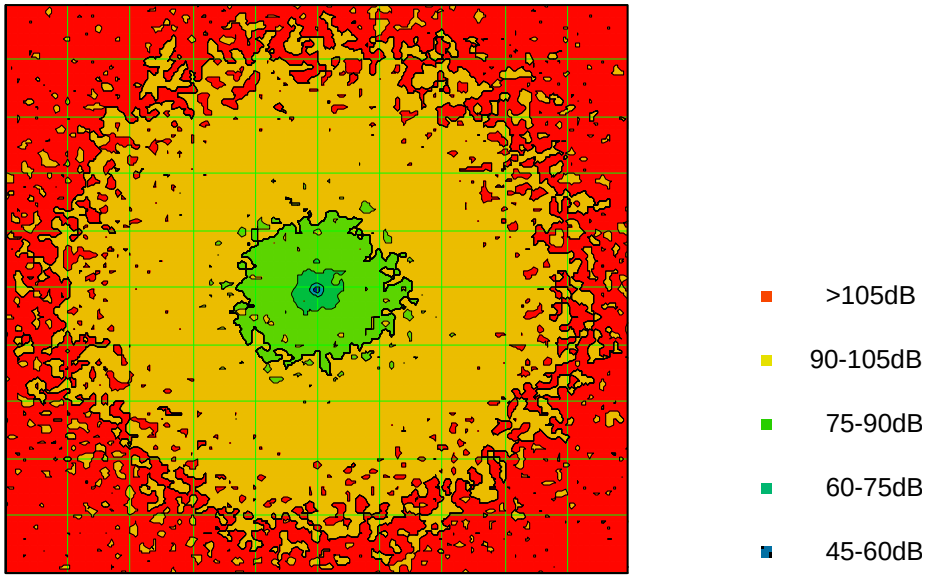

Figure 4.24 Propagation coverage simulation based on field measurements.

CHAPTER 5

MAPINFO ANALYSIS

MapInfo a desktop mapping software is used here as an analytical tool. This worldwide popular software is used widely in mobile communications system design. It basically gives a detailed map of any area of interest with an option to display secondary features such as municipals, railroads, rivers, water bodies, highways, streets and many more. In essence, this mapping tool gives a realistic picture of any simulated propagation coverage area. MapInfo makes this possible by allowing the user to import into its program a raster image with map coordinates.

5.1 Raster Image

A raster image is a type of computerized image that consists of row after row of tiny dots (pixels). MapInfo can read any of the following types of raster image files: JPEG, GIF, TIFF, PCX, BMP, TGA (Targa), and BIL (SPOT satellite). To register a raster image, specific map coordinates of longitude/latitude degrees are entered into the Image Registration dialog. On completion, this now registered image can be successfully displayed on a map. Note however, in using MapInfo, any location west of the prime

meridian has a negative longitude, and any location south of the equator has a negative latitude. Thus, 80 degrees West corresponds to the X value –80.

Figure 5.1 Positions of the mobile unit based on propagation measurements along Ives Dairy road displayed as a layer on a map.

MapInfo software reads an imported raster image, as a layer that can be reordered in a map comprised of contiguous layers. Two Mathcad images, depicted in Figures 4.20 and 4.24, were saved as Bitmap (BMP) files and imported into MapInfo. Figure 5.1

shows the positions of the mobile unit based on propagation measurements along the Ives Dairy road displayed as a layer on a map. There is however a small difference in the plotted DGPS positions and actual physical map locations with respect to the transmitter and mobile unit. This difference in displayed positions is as a direct result of truncation error in the grid simulation and the approximate DGPS readings that are referenced to a local area beacon.

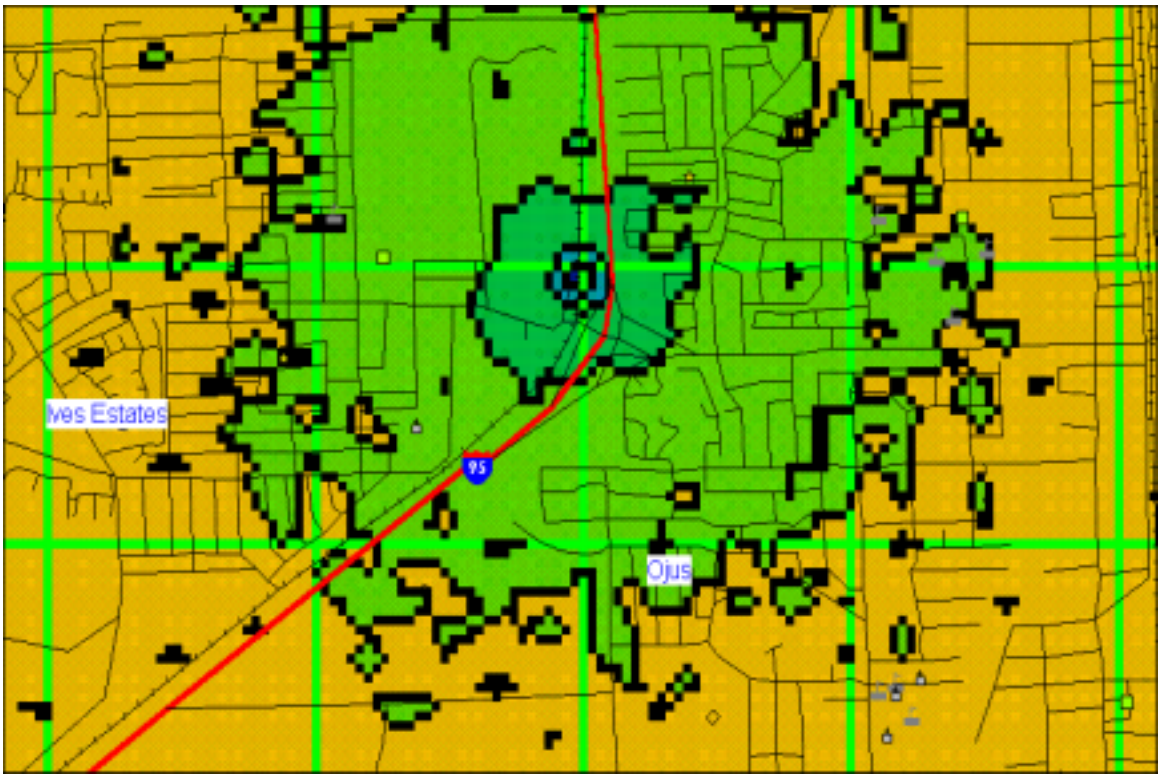

Figure 5.2 Propagation coverage simulation based on propagation measurements displayed as a layer on a map.

The simulated propagation coverage area displayed as a layer on a map is shown in Figure 5.2. This map image has been zoomed to show more or less the Ives Estates area. It gives a practical estimate of path loss at various points on the terrain. Based on Figure 4.24, this mapped area indicates a radial loss between 45 to 105 dB across the plane.

CHAPTER 6

COMSTUDY ANALYSIS

ComStudy is a RF propagation software, its base program is a geographic information system (GIS). ComStudy like MapInfo assembles information in layers (roads, cities etc.) and draws the layers on a map. ComStudy then adds other radio-related layers such as FCC databases of radio and television information, and proposed transmitter stations. This software calculates radio coverage for any located transmitter station using one of several built-in algorithms such as Longley-Rice, Bullington and Hata-Okumura. ComStudy also executes vertical path profiles (point-to-point) based on a single line drawn through two points on a map.

6.1 Vertical Path Profile

A vertical path profile shows the terrain along a path. ComStudy displays a path profile in a separate window. It gives the option of displaying the line-of-sight path, the first Fresnel zone, a possible diffraction path, or a combination of the three. The window default displays are the k-factor taken as *1.333*, with an exception for very long paths, and the Fresnel zone clearance of *0.600*. It gives site elevations in terms of distance

above mean sea level (AMSL) and tower or antenna heights as distance above ground level (AGL). ComStudy returns free space loss (as if no earth were present), plane earth loss (with the ground taken into consideration) and excess loss or diffraction loss.

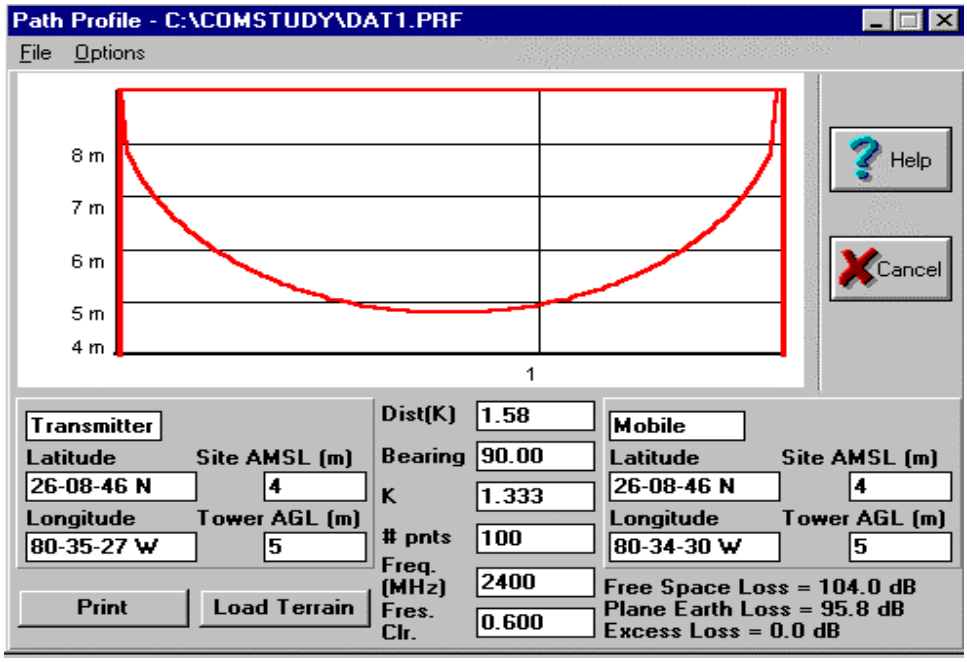

Figure 6.1 Vertical path profile taken between transmitter site and the farthest position of the mobile unit along Alligator alley.

A vertical path profile taken between the transmitter site and the farthest position of the mobile unit along Alligator alley is shown in Figure 6.1. The extent of the Fresnel zone area indicates that after approximately 800 meters the transmitted 2.4 GHz signal will begin to experience fading due to multipath effects. This is supported by the random

variations in measured signal strength, after a distance of 800 meters, displayed in the Mathcad generated scatter plot given as Figure 4.15. This problem could have been solved if there was a possibility to increase both antenna heights.

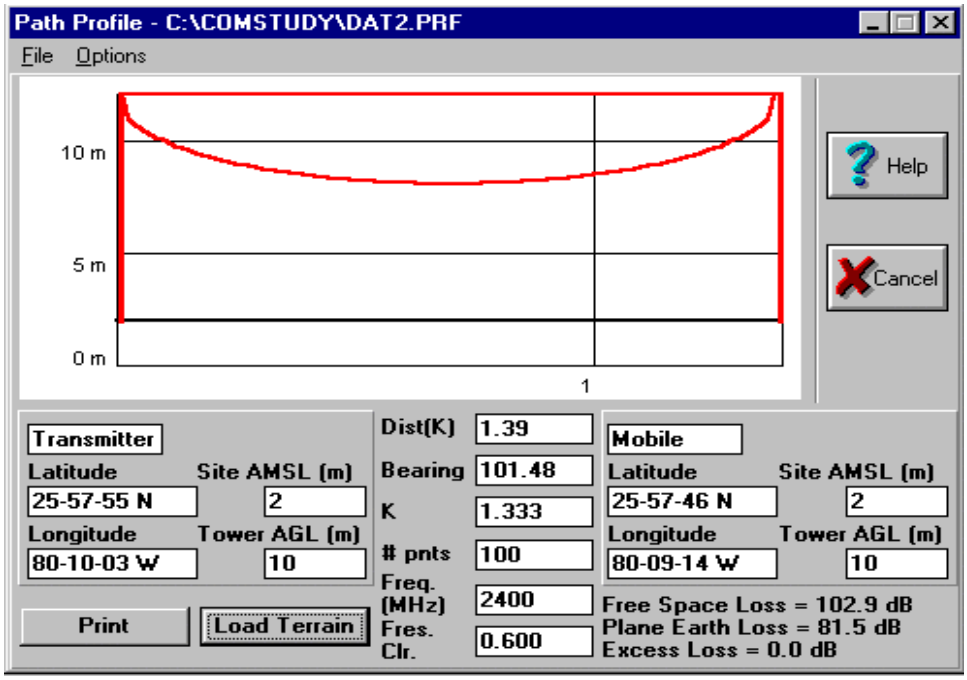

Figure 6.2 Vertical path profile taken between transmitter site and the farthest position of the mobile unit along Ives Dairy road.

The vertical path profile taken between transmitter site and the farthest position of the mobile unit along Ives Dairy road is shown in Figure 6.2. The extent of the Fresnel zone area indicates that there was adequate Fresnel zone clearance during the propagation measurements, since the receiving antenna was always elevated well above the trees in its immediate path.

CHAPTER 7

CONCLUSIONS

This thesis presented an innovative approach to RF propagation modeling for the spread spectrum environment. The development of a Mathcad model systematic approach to coverage prediction has been described. The Mathcad model consisted of a terrain database, a propagation prediction model, and a subsystem of various Mathcad programs to simulate coverage patterns in terms of path loss and bit error rate. MapInfo and ComStudy software were used as analytic tools.

Accurate modeling of RF propagation is of vital importance in every stage of communications system design. For this reason, a propagation model should be optimized to accurately reflect the propagation characteristics of the particular environment. To this effect, the propagation prediction model presented, based on the Miami propagation measurements, should be improved. Propagation measurements are needed for every facet of radio coverage, such as with variable transmitting and receiving antenna heights, with the effects of clutter, and the effects of buildings. As such the path loss constants obtained using regression analysis can be optimized, resulting in an established path loss empirical formula.

The accurate prediction of coverage BER in multipath channels is becoming increasingly important in communications system design as the demand grows for digital wireless systems. BER predictions allow designers to determine acceptable modulation methods, coding techniques and receiver implementations in the operating environments. The BER simulation method presented, using link analysis, is indeed a big step forward. It provides the maximum allowable path loss that can be tolerated on the radio link and as such determines the extent of acceptable cell coverage radius.

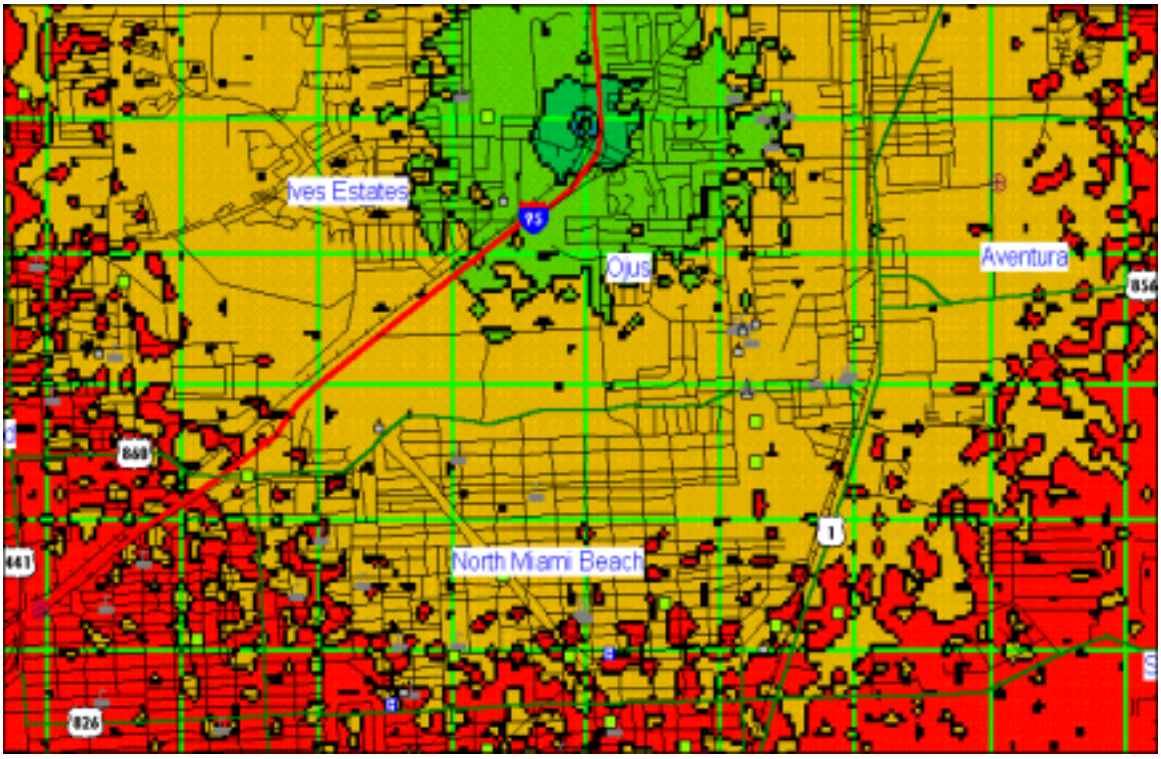

Figure 7.1 Propagation prediction coverage simulation based on propagation measurements displayed as a layer on a map over a 5 km radius.

Figure 5.2 showed the propagation coverage simulation based on propagation measurements displayed as a layer on a map over a 2 km radius. The propagation prediction coverage simulation over a 5 km radius is shown in Figure 7.1, transmitting the 2.4 GHz carrier. If digital modulation was used a similar simulation can show predicted average BER as a function of path loss.

The Mathcad model has been shown to be a practical method of simulating propagation coverage. However, if propagation coverage is limited to the microcell level, say a 1×1 km square map, a 101×101 path loss matrix will result in a grid resolution of 1/50 km or 20 meters, producing far more accurate simulations. Overall, this Mathcad model approach can in the future provide a speedy and economic service to communications system design engineers.

LIST OF REFERENCES

1. G. E. Chan, “Propagation and Coverage Prediction for Cellular Radio Systems,” IEEE Trans. on Veh. Technol., vol. 40, pp. 665-670, November 1991.

2. M. Hata, “Empirical Formula for Propagation Loss in Land Mobile Radio Services,” IEEE Trans. on Veh. Technol., vol. VT-29, pp. 317-325, August 1980.

3. T. S. Rappaport, “Wireless Communications: Principles and Practice,” IEEE Press, Prentice-Hall, New Jersey, 1996.

4. P. T. Chien and H. S. Loke, “Overview of Spread Spectrum Communications,” http://www.cwc.nus.sg/cwcdocs/newsletter/sscomm.htm, December 1997.

5. R. L. Peterson, R. E. Ziemer and D. E. Borth, “Introduction to Spread Spectrum Communications,” Prentice-Hall, New Jersey, 1995.

6. A. A. R. Townsend, “Digital Line-of-sight Radio Links: A Handbook,” Prentice-Hall, London, 1988.

7. J. D. Gibson, “The Mobile Communications Handbook,” CRC Press, Boca Raton, Florida, 1996.

8. J-P. M. G. Linnartz, “Wireless Communications: Propagation Channels: Path Loss,” http://ns.baltzer.nl/wirelesscd/diffrac.htm, November 1997.

9. A. G. Longley and P. L. Rice, “Prediction of Tropospheric Radio Transmission Loss Over Irregular Terrain: A Computer Method,” ESSA Tech. Rep. ERL 79 – ITS 67, US Govt. Printing Office, Washington DC, 1968.

10. W. C. Jakes, “Microwave Mobile Communications,” IEEE Press, New Jersey, 1974.

11. J. Walfisch and H. L. Bertoni, “A Theoretical Model of UHF Propagation in Urban Environments,” IEEE Trans. on Antennas Propagat., vol. 36, pp. 1788-1796, December 1988.

12. V. K. Garg, K. F. Smolik and J. E. Wilkes, “Applications of CDMA in Wireless/Personal Communications,” Prentice-Hall, New Jersey, 1997.

13. B. Sklar, “Digital Communications: Fundamentals and Applications,” Prentice-Hall, New Jersey, 1988.

14. E. H. Dinan and B. Jabbari, “Spreading Codes for Direct Sequence CDMA and Wideband CDMA Cellular Network,” IEEE Commun. Mag., vol. 36, pp. 48-54, September 1998.

15. L. Chew, “Maps: Coordinate Systems,” GPS Workshop Manual, 1998.